Supplementary Information (SI) for Physical Chemistry Chemical Physics.
This journal is © the Owner Societies 2026

Electronic supplementary information

Aggregation-induced and stimuli-responsive emission modulation in pyridil-imidazole compounds connected to naphthalene, anthracene and pyrene for the design of sensors and switches

Tuhin Abedin[†], Raju Biswas[†], Sourav Mardanya[†‡], and Sujoy Baitalik[*†]

[†]Department of Chemistry, Inorganic Chemistry Section, Jadavpur University, Kolkata 700032, India.

[‡] Department of Chemistry, Deshabandhu Mahavidyalaya, Paschim Bardhaman, West Bengal, Pin-713331, India

[*] *To whom correspondence should be addressed: E-mail: sbaitalik@hotmail.com, sujoy.baitalik@jadavpuruniversity.in*

Table of contents

1.1 Synthesis of the compounds

The general procedure followed for the synthesis of the desired compounds is described below.

2-(2-(naphthalen-2-yl)-5-(pyridin-2-yl)-1H-imidazol-4-yl) pyridine (dipy-phimz-naphthalen): 2,2'-Pyridil (100 mg, 0.47 mmol) and 2-naphthaldehyde (73 mg, 0.47 mmol) were dissolved in 50 mL of chloroform. Ammonium acetate (8.5 g) and acetic acid (10 mL) were added to this solution, and the mixture was refluxed for approximately 5 h. After cooling to room temperature, the reaction mixture was neutralized by the dropwise addition of a saturated sodium carbonate solution. The organic layer was separated using a separating funnel, and the solvent was removed under reduced pressure using a rotary evaporator. The crude product was purified by recrystallization from a 1:1 ethanol-methanol mixture, yielding the desired compound. Yield: 178 mg (51%). Elemental Anal. Calcd for $C_{24}H_{19}N_4$: C, 79.31; H, 5.27; N, 15.42. Found: C, 79.19; H, 5.23; N, 15.11. ^{1}H NMR (400 MHz, DMSO-d_6): δ/ppm 10.80 (*s*, N-H), 9.12 (*d*, 2H, *J*=4Hz, $2H_6$), 8.78 (*s*, 1H, *J*=8Hz, H_9), 8.69(*d*, 2H, *J*=8Hz, $2H_3$), 8.48 (*t*, 2H, *J*=8Hz, $2H_5$), 8.33(*d*, 1H, *J*=12Hz, H_{14}), 8.12 (*d*, 1H, *J*=12Hz, H_{13}). 8.05 (m, 1H, *J*=12Hz, H_{12}), 8.01 (m, 1H, *J*=4 Hz, H_{11}), 7.86 (t, 2H, *J*=8.0 Hz, $2H_4$), 7.63 (m, 1H, *J*=4.0 Hz, H_{10}), ESI-MS (positive, MeCN) m/z = 349.1454 (100%) [(**1**+H^+)]. ^{13}C NMR (400 MHz, DMSO) δ: 149.20, 145.64, 144.13, 143.00, 133.67, 132.77, 128.88, 128.70, 128.18, 127.82, 127.49, 125.95, 125.72, 124.83, 123.85, 123.16, 39.93, 39.72, 39.51, 39.30, 39.09, 38.88, 38.67.

2-(2-(anthracen-9-yl)-5-(pyridin-2-yl)-1H-imidazol-4-yl) pyridine (dipy-phimz-anthracen): The compound is synthesized by adopting the same procedure as above, except by using 9-anthracenealdehyde (97 mg, 0.47 mmol) in place of 2-napthaldehyde. Yield: 239 mg (56%). Elemental anal. Calcd. for $C_{27}H_{18}N_4$: C, 81.39; H, 4.55; N, 14.06. Found: C,

81.22; H, 4.45; N, 13.80. ^{1}H NMR (400 MHz, DMSO-d_6): δ/ppm 11.40 (*s*, N-H), 9.20 (*d*, 2H, *J*=4Hz, $2H_6$), 8.95 (*S*, 1H, *J*=12Hz, H_{13}), 8.55 (*s*, 1H, *J*=8Hz, $1H_9$), 8.44 (*t*, 2H, *J*=8Hz, $2H_5$), 8.28 (*d*, 2H, *J*=12Hz, $2H_3$), 7.89 (*t*, 2H, *J*=8Hz, H_4). 7.81 (d, 1H, *J*=8Hz, H_{12}), 7.62 (m, 2H, *J*=8 Hz, H_{10} +H_{11}), ESI-MS (positive, MeCN) m/z = 399.1611 (100%) [(**2**+H^+)]. ^{13}C NMR (400 MHz, DMSO) δ: 194.79, 147.60, 146.19, 144.51, 143.37, 135.86, 131.26, 131.05, 130.07, 129.96, 129.81, 129.13, 127.89, 126.41, 126.38, 125.48, 124.97, 123.72, 123.67, 123.15, 39.89, 39.68, 39.47, 39.26, 39.05, 38.84, 38.63.

2-(2-(pyren-8-yl)-5-(pyridin-2-yl)-1H-imidazol-4-yl)pyridine (dipy-phimz-pyren):

The compound is synthesized by adopting the same procedure as above, except by using 1-Pyrenecarboxaldehyde (108 mg, 0.47 mmol) in place of 2-napthaldehyde. Yield: 241 mg (57%). Elemental anal. Calcd. for $C_{29}H_{20}N_4$: C, 82.05; H, 4.75; N, 13.20. Found: C, 81.92; H, 4.67; N, 13.04. ^{1}H NMR (400 MHz, DMSO-d6): δ/ppm 10.85 (*s*, N-H), 9.15 (d, 2H, J=4Hz, $2H_6$), 9.12 (d, 1H, J=12Hz, H_{17}), 8.68 (d, 1H, J=8Hz, $1H_{16}$), 8.58 (d, 2H, J=8Hz, $2H_3$), 8.47 (m, 3H, J=8Hz,4Hz, $H_{11,}$ $H_{12,}$ H_{13}), 8.35 (m, 4H, J=,4Hz,8Hz,12Hz, H_9, $H_{10,}$ $H_{14,}$ H_{15}). 8.17 (t, 2H, J=8Hz, $2H_5$), 7.89 (t, 2H, J=8 Hz, H_4), ESI-MS (positive, MeCN) m/z = 423.1609 (100%) [(**3**+H+)]. ^{13}C NMR (400 MHz, DMSO) δ: 194.28, 149.68, 143.17, 132.37, 131.26, 130.64, 129.30, 129.24, 129.10, 128.05, 127.74, 127.28, 126.63, 126.27, 125.26, 125.15, 124.90, 124.54, 123.97, 123.44, 123.14, 40.45, 40.24, 40.14, 40.03, 39.82, 39.61, 39.40, 39.20.

2. Experimental section

2.1 Physical measurements

^{1}H-NMR spectra were recorded using a Bruker Avance DPX 400MHz spectrometer with DMSO-d_6 as the solvent. HRMS data were acquired from Waters mass spectrometer. Infrared spectra of the compounds were recorded in the range of 4000 cm^{-1} to 400 cm^{-1} with a Perkin-Elmer FT-IR spectrometer (spectrum two) with the samples following the attenuated total reflectance (ATR) technique. Elemental analyses of the compounds were performed with a Vario-Micro V2.0.11 elemental (CHNSO) analyzer. UV-visible absorption spectra were measured using a Shimadzu UV-1800 spectrophotometer. Steady-state fluorescence emission spectra were acquired on a HORIBA fluoromax-4 spectrometer. Luminescence lifetimes were measured at room temperature using the time-correlated single-photon counting (TCSPC) technique. For TCSPC measurements, photoexcitation was performed at 355 nm using a nanosecond diode laser. The luminescence decay data were collected with a Hamamatsu MCP photomultiplier (R3809) and analyzed using IBH DAS6 software. All solvatochromic photophysical studies were conducted using compounds at concentrations of approximately ~2×10^{-5} M. The relative quantum yields of all four compounds (**1-3**) at room temperature were measured, using quinine sulfate in 1 N H_2SO_4 (η = 1.338, Φr = 54.6%) as the reference. The quantum yields were calculated using a general equation (S1) where 'r' denotes the reference and 's' the sample. In this equation, 'A' refers to the absorbance at the excitation wavelength, 'I' represents the integrated luminescence intensity, and 'η' is the refractive index of the solvent. SEM data were recorded in a FEI INSPECT F50 instrument.

$$\frac{\Phi_s}{\Phi r} = \frac{A_r \eta_s^2 I_s}{A_s \eta_r^2 I_r} \qquad \text{.....(S1)}$$

2.2 Computational details

All calculations were performed with the Gaussian 09 program[S1] package employing the DFT method with Becke's three-parameter hybrid functional and Lee-Yang-Parr's gradient corrected correlation functional (B3LYP) level of theory using 631-G basis set for the ligands[S2,S3] dipy-phimz-X (**1-3**). To compute the UV-vis absorption transitions of the compounds, the singlet state geometries corresponding to the vertical excitations were optimized using the time-dependent DFT (TD-DFT) scheme starting with the ground state geometries optimized in solution phase.[S4-S9] Orbital and fractional contribution analysis were done with Gauss View [S10] and Gauss Sum 2.1.[S11]

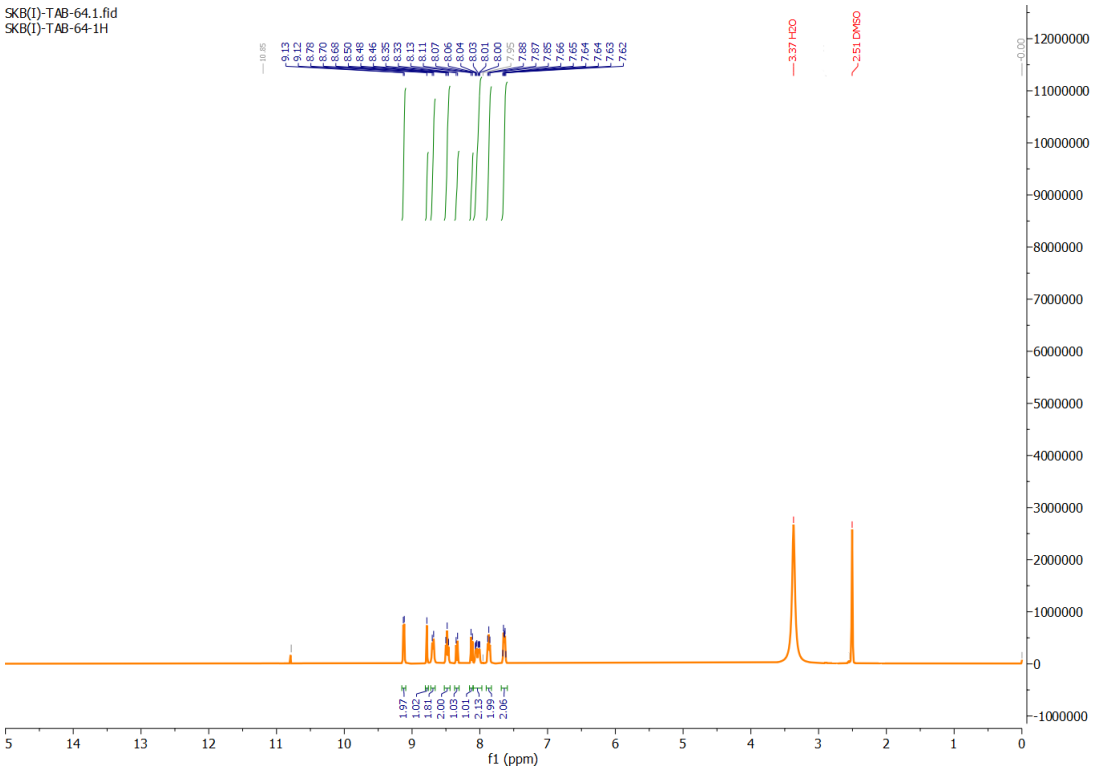

Fig. S1 Full range ^{1}H-NMR (400MHz) spectrum of **1** in DMSO-d_6.

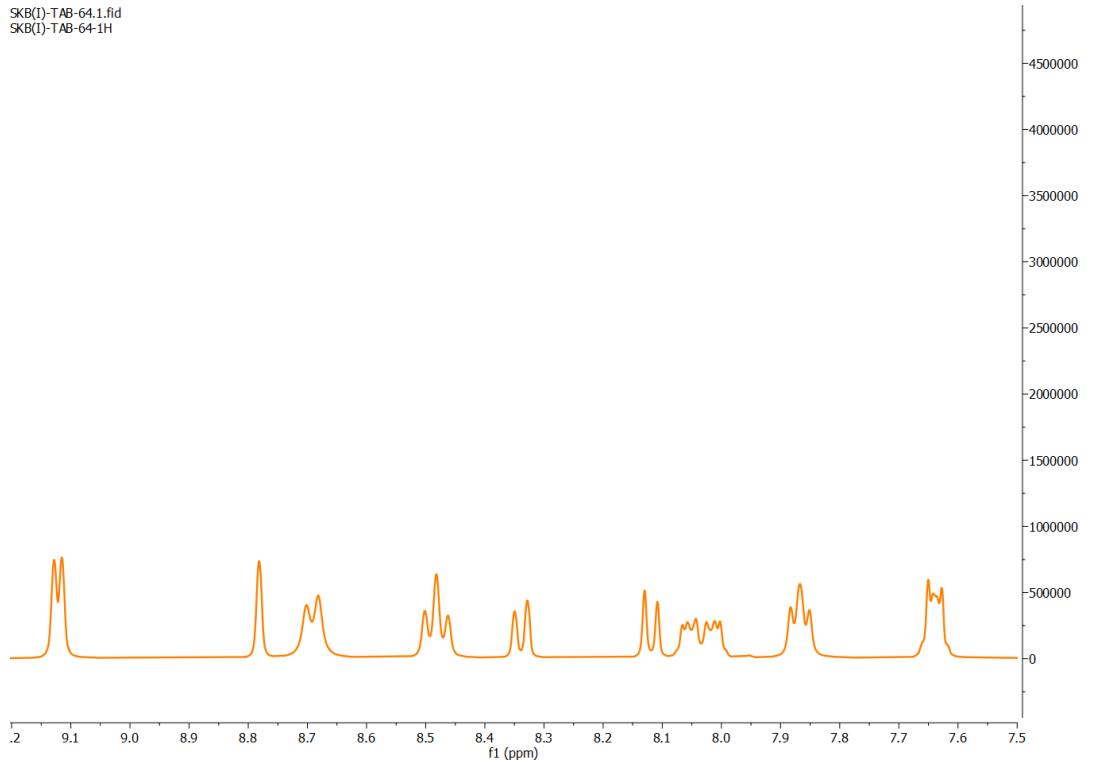

Fig. S2 Expanded ^{1}H-NMR (400MHz) spectrum of **1** in DMSO-d_6.

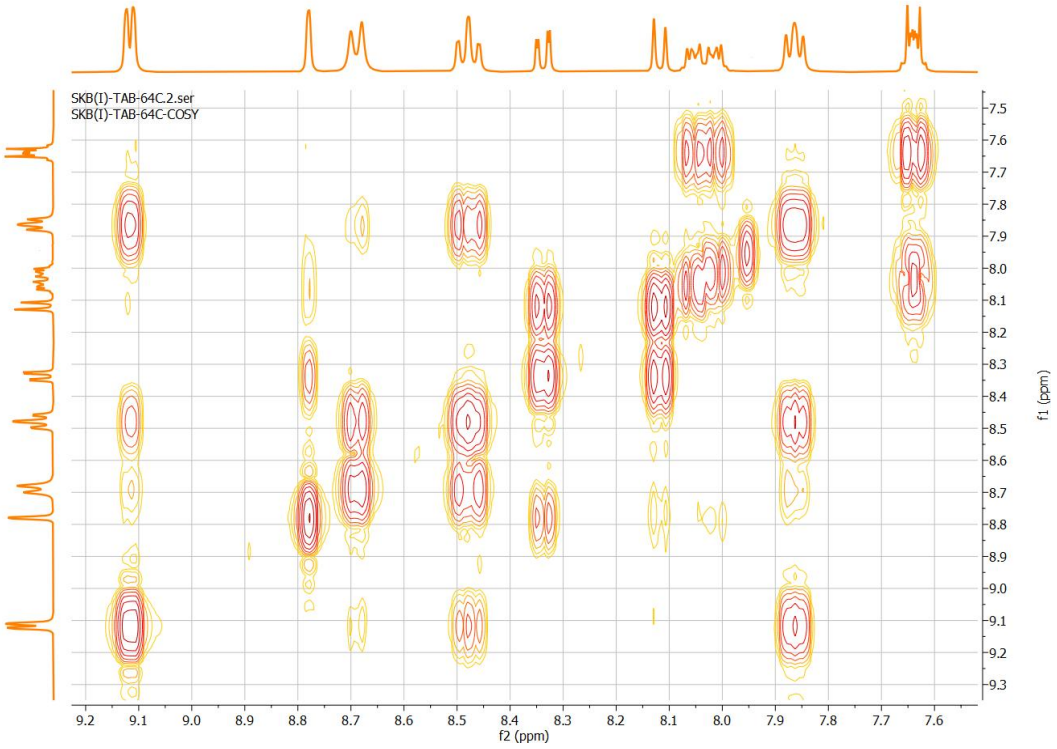

Fig. S3 {^{1}H–^{1}H} COSY NMR spectrum of **1** in DMSO-d_6.

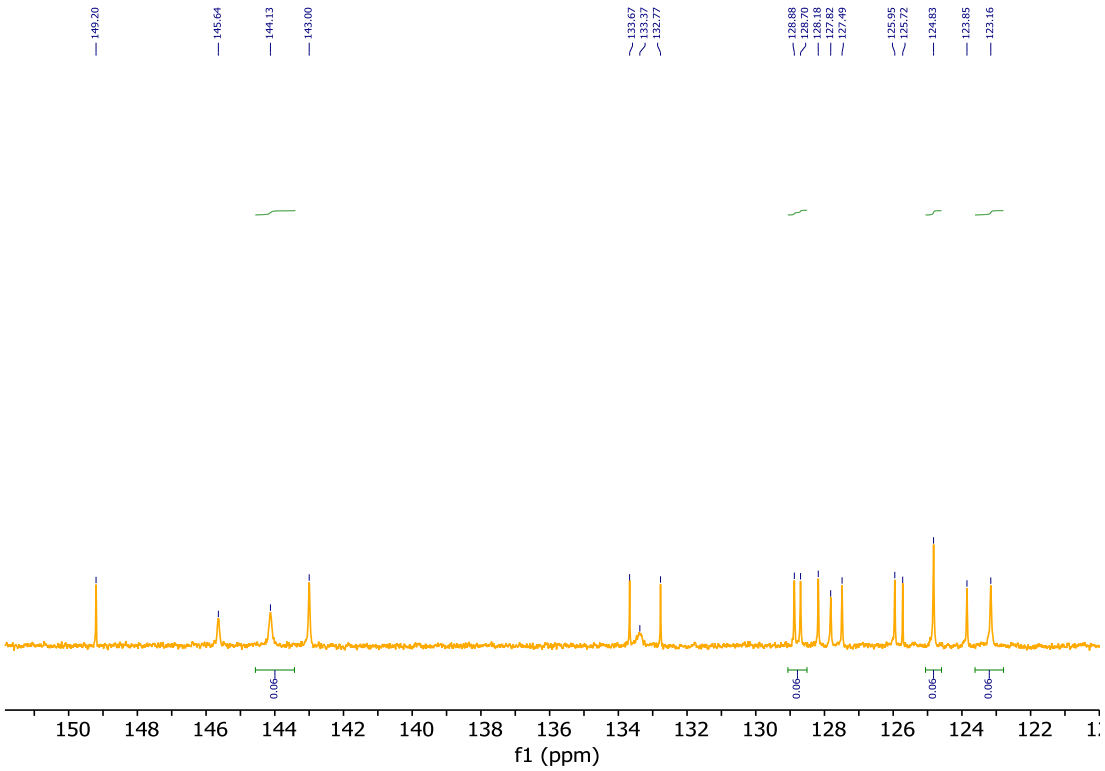

Fig. S4 ^{13}C NMR spectrum of **1** in DMSO-d_6.

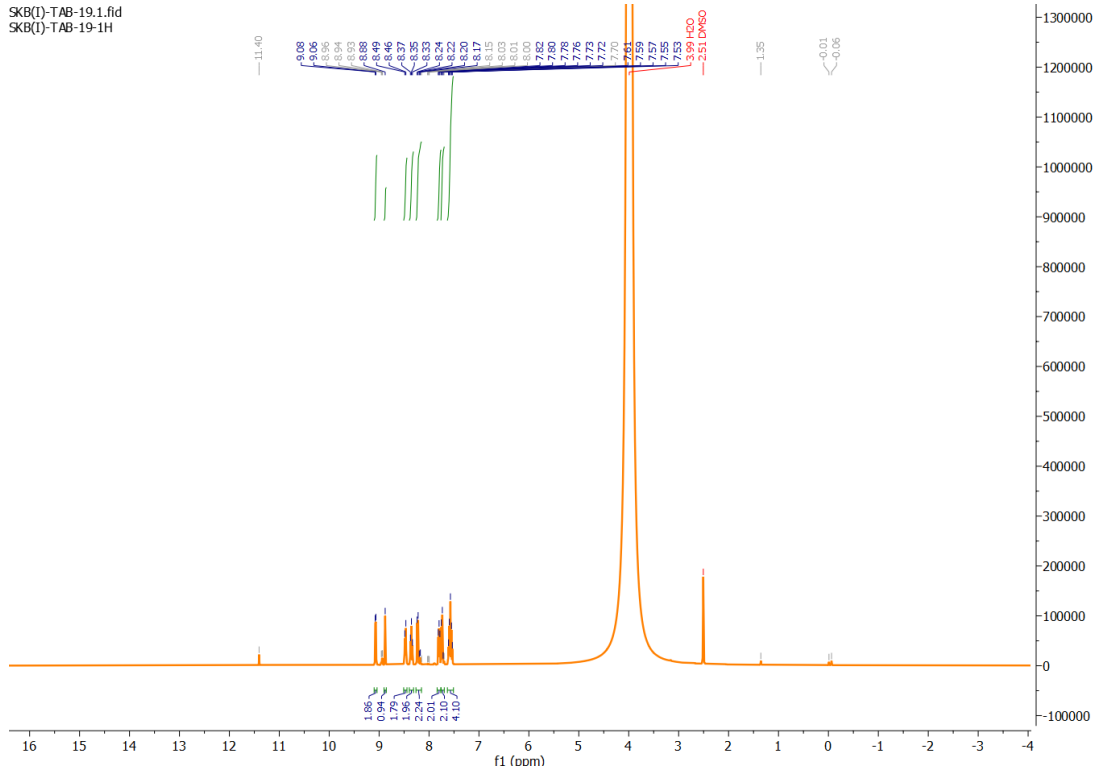

Fig. S5 Full range ^{1}H-NMR (400MHz) spectrum of **2** in DMSO-d_6.

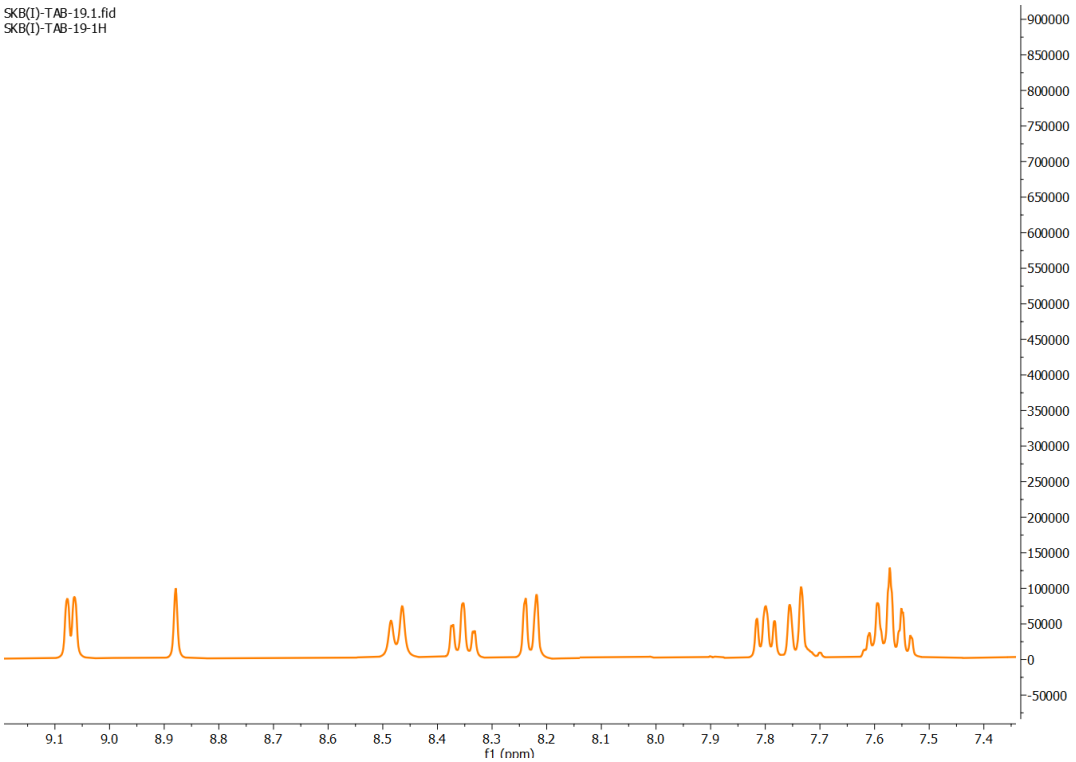

Fig. S6 Expanded ^{1}H-NMR (400MHz) spectrum of **2** in DMSO-d_6.

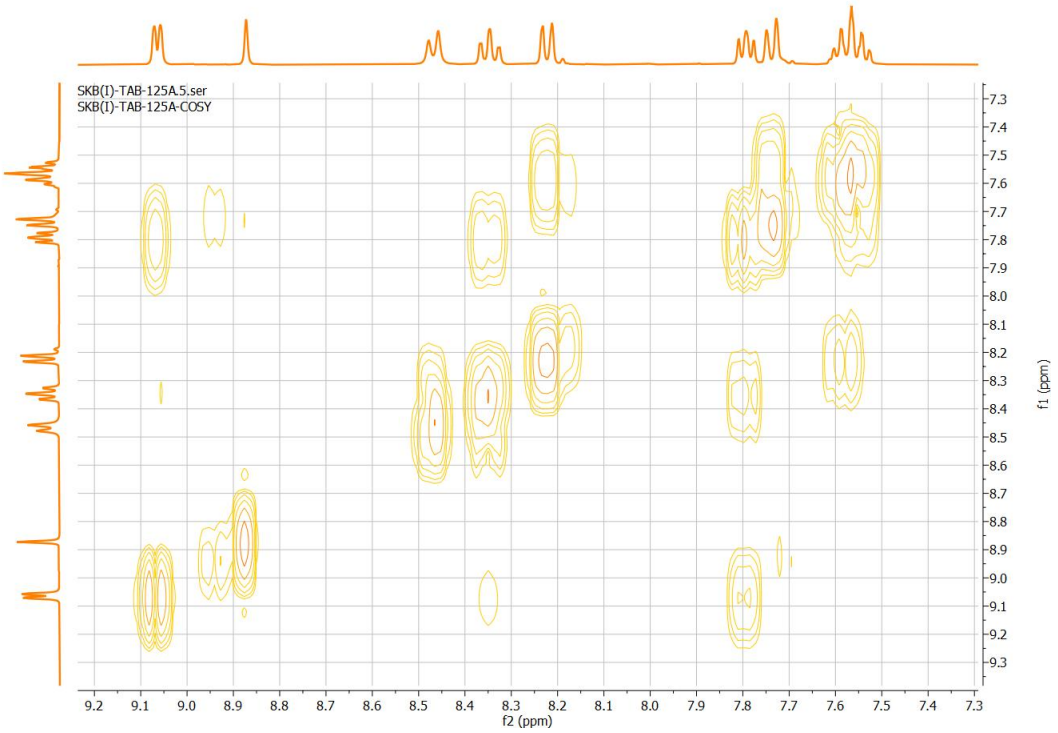

Fig. S7 {^{1}H–^{1}H} COSY NMR spectrum of **2** in DMSO-d_6.

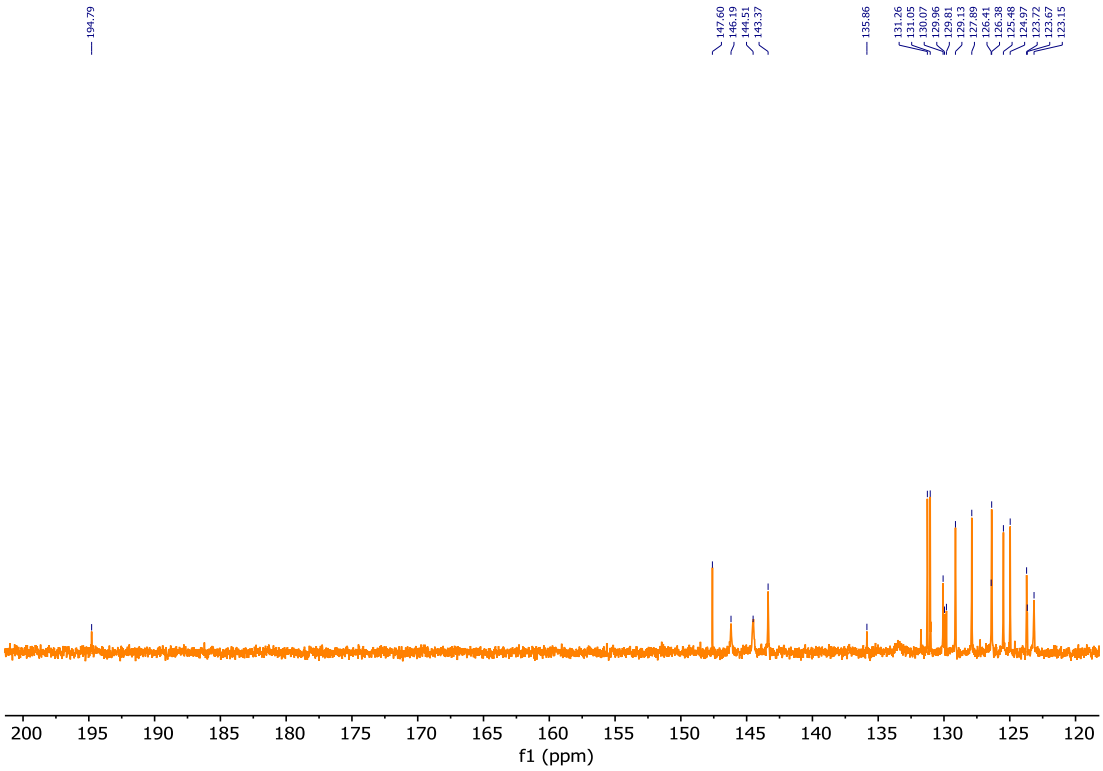

Fig. S8 ^{13}C NMR spectrum of **2** in DMSO-d_6.

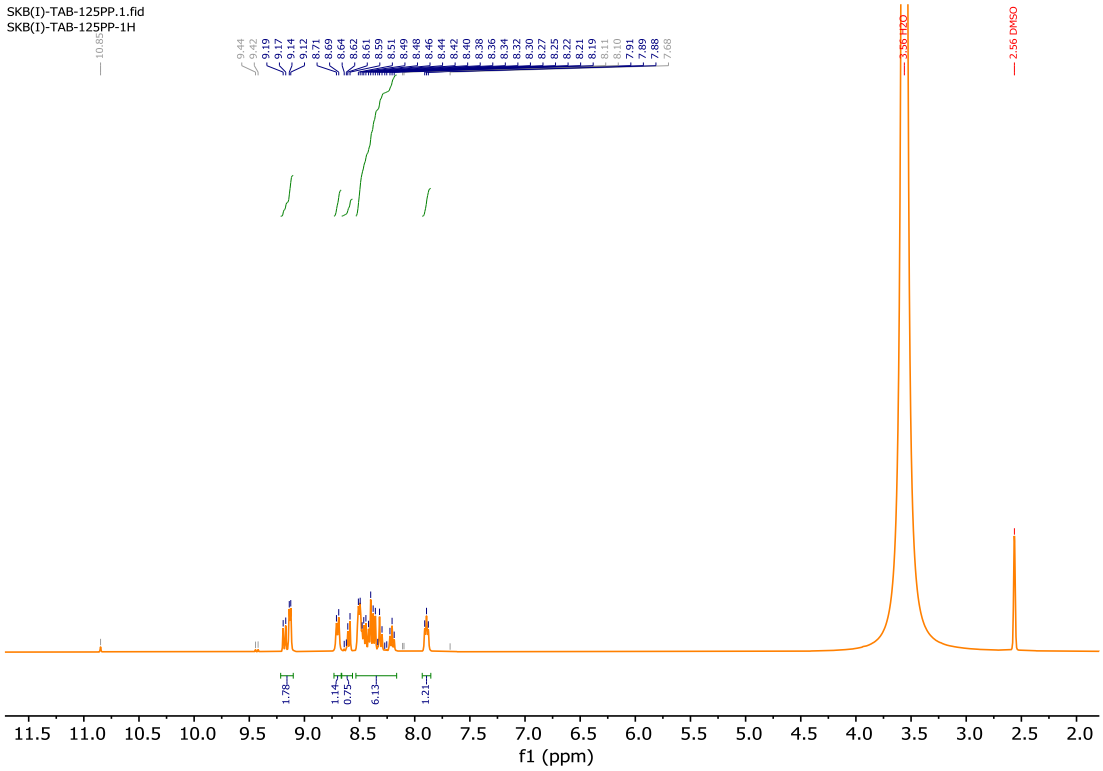

Fig. S9 Full range ^{1}H-NMR (400MHz) spectrum of **3** in DMSO-d_6.

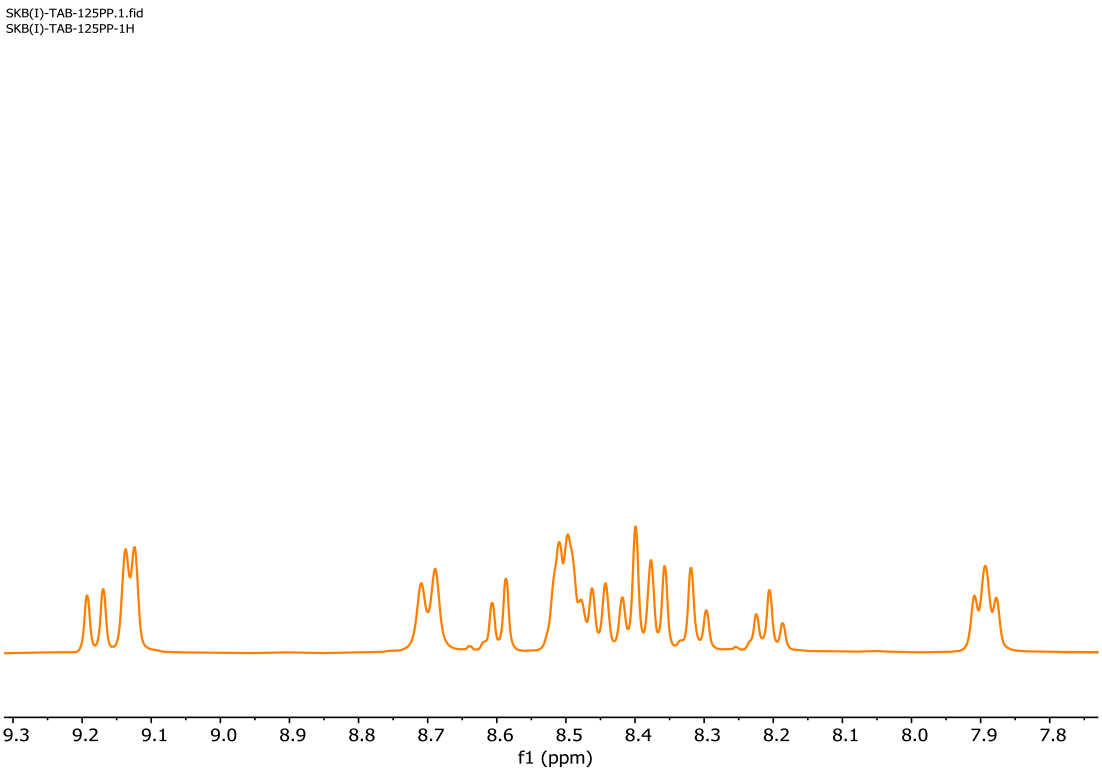

Fig. S10 Expanded ^{1}H-NMR (400MHz) spectrum of **3** in DMSO-d_6.

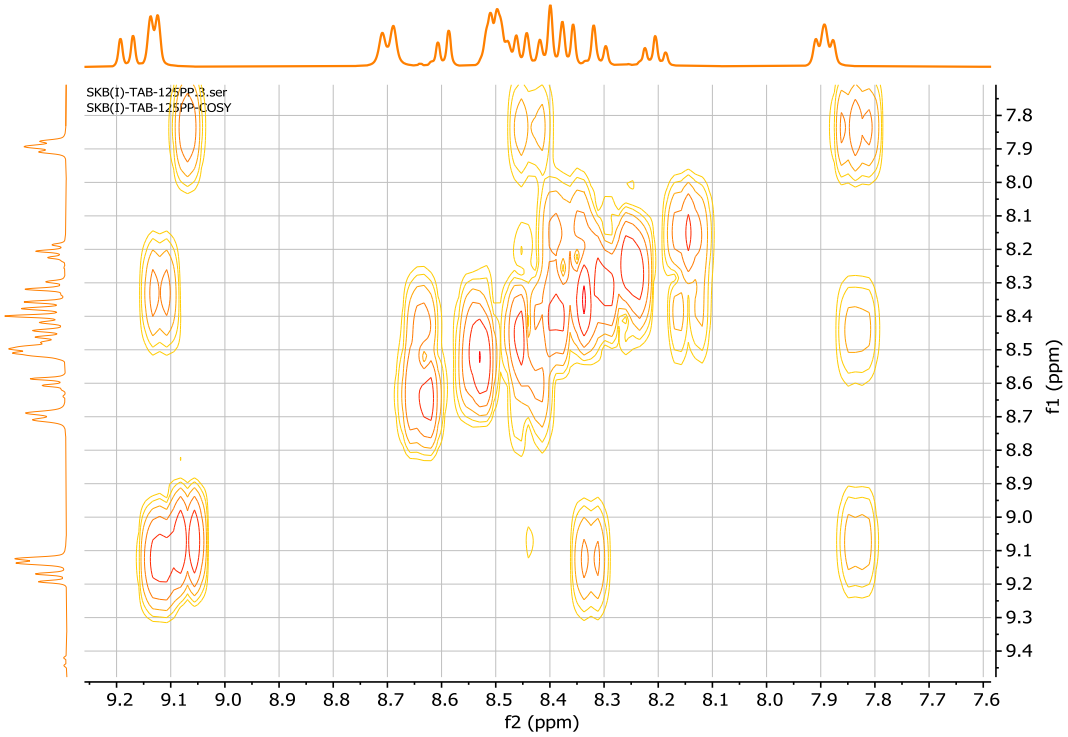

Fig. S11 {^{1}H–^{1}H} COSY NMR spectrum of **3** in DMSO-d_6.

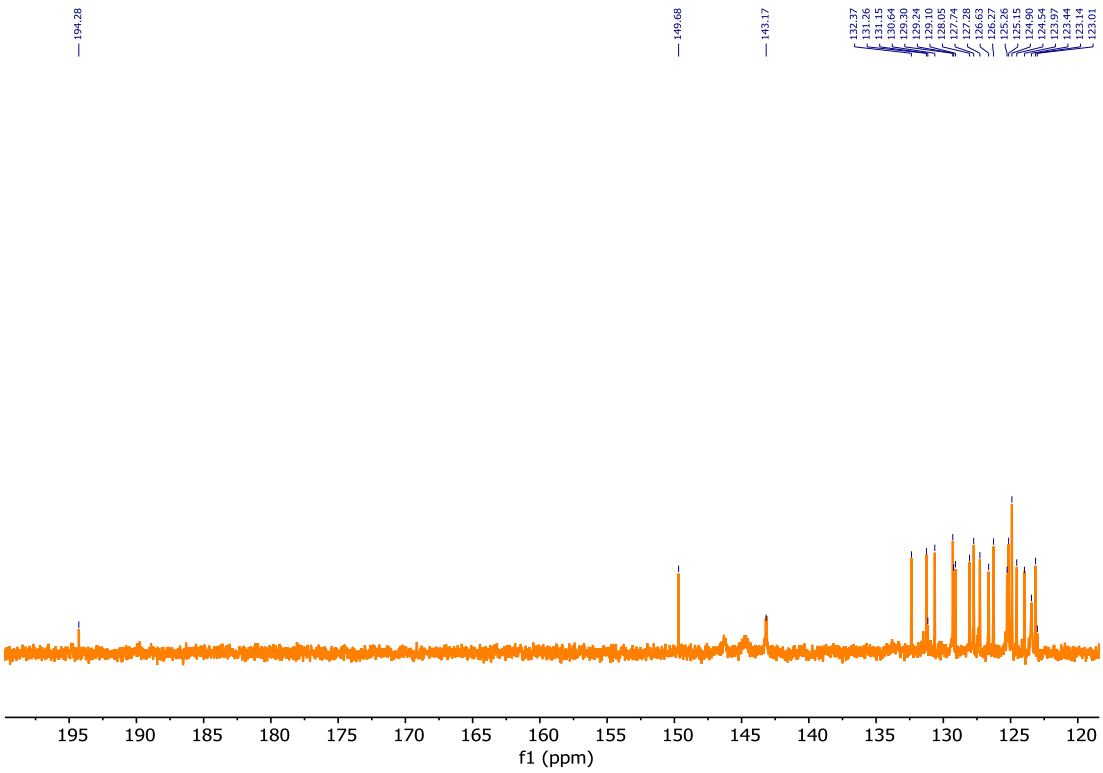

Fig. S12 ^{13}C NMR spectrum of **3** in DMSO-d_6.

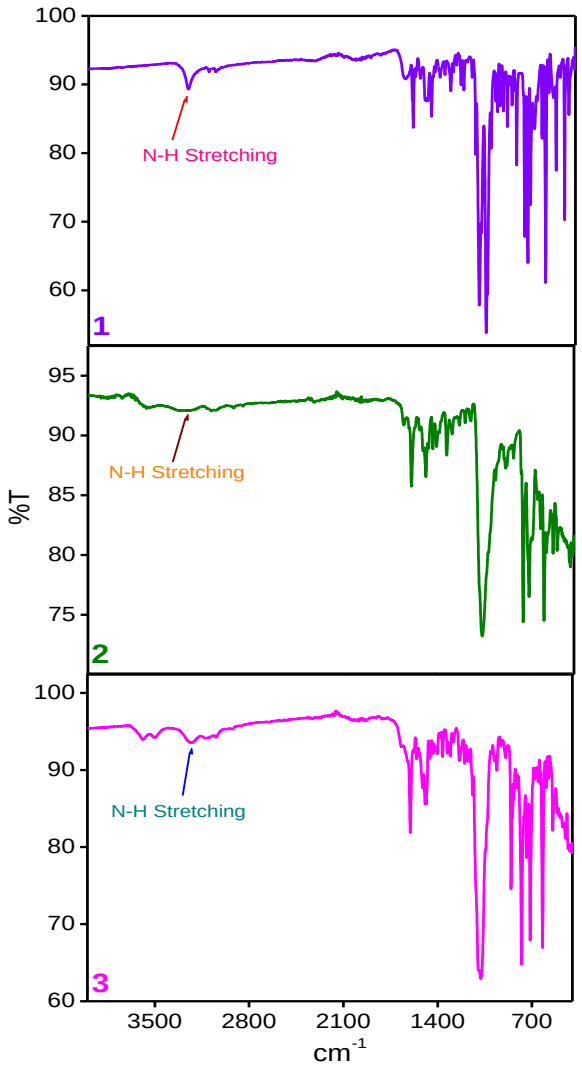

Fig. S13 FT-IR spectrum of compound **1-3**.

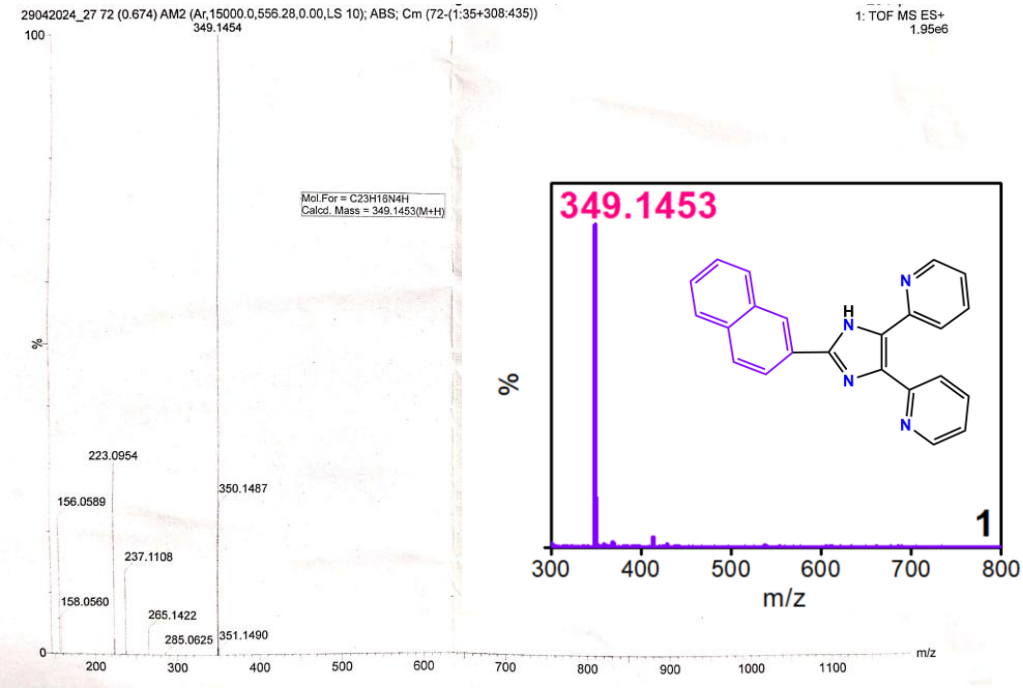

Fig. S14 HRMS spectrum (positive) of **1** (m/z=349.1453) in MeCN.

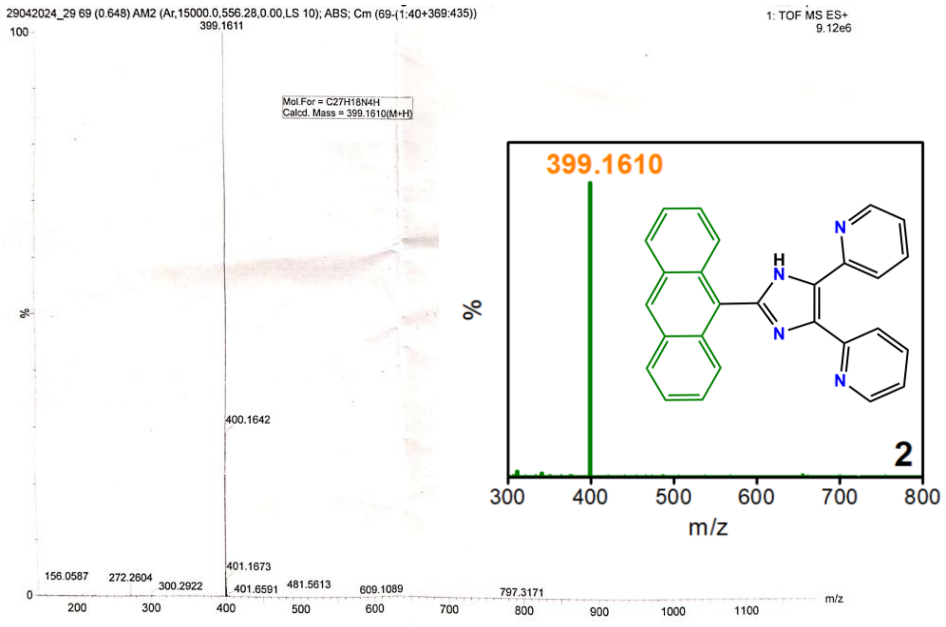

Fig. S15 HRMS spectrum (positive) of **2** (m/z=399.1610) in MeCN.

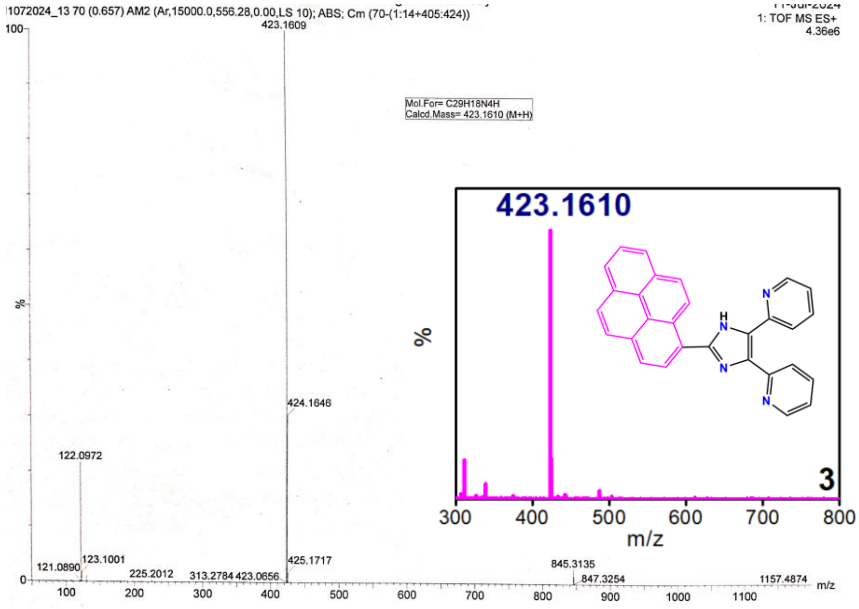

Fig. S16 HRMS spectrum (positive) of **3** (m/z=423.1610) in MeCN.

Table S1 Composition table of compound **1**

MO	*py-imz-naphthalene* (***1***)				
	Energy/ev		% of compositions		
			Naphthalene	imidazole	pyridil
LUMO+5	0.05		17.28	6.47	76.24
LUMO+4	-0.53		5.44	1.59	92.95
LUMO+3	-0.60		1.01	1.37	97.61
LUMO+2	-0.76		75.26	9.11	15.62
LUMO+1	-1.38		59.29	14.28	26.41
LUMO	-1.61		23.58	25.71	50.70
HOMO	-5.44		31.98	42.72	25.28
HOMO-1	-6.16		80.91	7.99	11.09
HOMO-2	-6.82		49.91	14.47	35.61
HOMO-3	-6.96		0.10	7.41	92.48
HOMO-4	-7.03		28.51	20.65	50.82
HOMO-5	-7.34		0.29	14.88	84.81

Table S2 Composition table of compound **2**

MO	*py-imz-anthracene* (***2***)				
	Energy/ev		% of compositions		
			Anthracene	Pyridil	imidazole
LUMO+5	-0.23		11.16	71.43	17.40
LUMO+4	-0.54		92.67	6.86	0.45
LUMO+3	-0.56		5.91	92.19	1.89
LUMO+2	-0.62		2.79	92.83	4.37
LUMO+1	-1.53		2.40	71.90	25.68
LUMO	-1.97		94.00	2.50	3.93
HOMO	-5.33		73.69	9.07	17.23
HOMO-1	-5.91		27.51	35.88	36.60
HOMO-2	-6.71		99.36	0.26	0.36
HOMO-3	-6.94		10.31	59.69	29.97
HOMO-4	-6.96		00.37	90.74	8.87
HOMO-5	-7.10		88.61	8.46	2.91

Table S3 Composition table of compound **3**

MO	*py-imz-pyrene* (***3***)			
	Energy/ev	% of compositions		
		Pyridyl	pyrene	imidazole
LUMO+5	-0.31	25.11	67.58	7.29
LUMO+4	-0.56	94.87	3.41	1.71
LUMO+3	-0.61	95.33	1.93	2.72
LUMO+2	-0.90	3.28	93.83	2.88
LUMO+1	-1.51	67.40	9.33	23.26
LUMO	-1.90	7.44	81.34	11.21
HOMO	-5.27	12.71	62.58	24.70
HOMO-1	-5.96	27.61	45.84	26.54
HOMO-2	-6.49	4.50	93.25	2.23
HOMO-3	-6.94	60.76	9.90	29.32
HOMO-4	-6.97	90.21	0.84	8.94
HOMO-5	-7.05	6.42	91.27	2.29

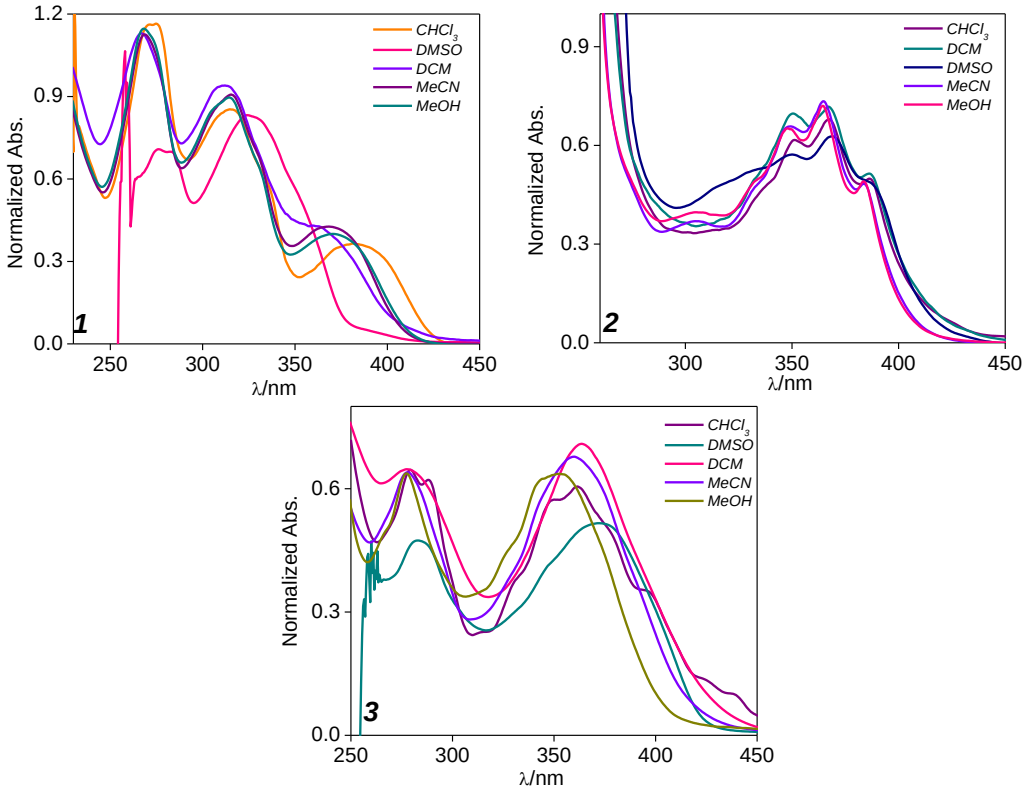

Fig. S17 UV-vis absorption spectra of **1-3** in different solvents.

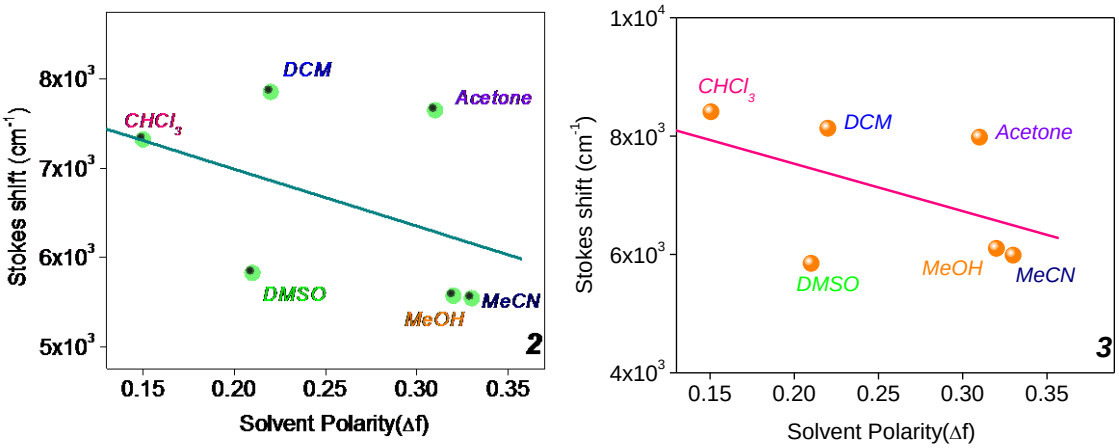

Fig. S18 Lippert-Mataga plot showing Stokes shift (Δν) against solvent polarity parameter (Δf) of compound **2** and **3**.

Table S4 Selected UV-vis energy transitions at the TD-DFT/B3LYP level of **1** in MeCN

λ_{exp} /nm	Excited State	λ_{cal} /nm	Oscillator strength	Key transitions	Character
py-imz-naphthalene (***1***)					
372	S1	357	0.73	HOMO→LUMO (98%)	ICT
270	S9	266	0.28	H-2→LUMO (61%), H-1→L+2 (16%)	ICT, π -π*
225	S24	225	0.09	H-2→L+3 (16%), HOMO→L+6 (13%), H-6→L+1 (10%)	ICT, π -π*

Table S5 Selected UV-vis energy transitions at the TD-DFT/B3LYP level of **2** in MeCN

λ_{exp} /nm	Excited State	λ_{cal} /nm	Oscillator strength	Key transitions	Character
py-imz-anthracene (***2***)					
384	S1	419	0.26	H→L (98%)	π -π*
348	S5	313	0.05	H-1→L+1(97%)	ICT
253	S22	242	0.02	H-5→L+1(76%)	ICT

Table S6 Selected UV-vis energy transitions at the TD-DFT/B3LYP level of **3** in MeCN

λ_{exp} /nm	Excited State	λ_{cal} /nm	Oscillator strength	Key transitions	Character
py-imz-pyrene (***3***)					
360	S1	406	0.923	HOMO→LUMO (97%)	π -π*
278	S6	296	0.178	H→L+2 (11%), H→L+3 (37%), H→L+4 (21%)	ICT, π -π*
233	S29	233	0.201	H-2→L+2 (35%), H-1→L+6 (16%)	π -π*
198	S69	193	0.186	H-9→L+2 (22%), H-8→L+2 (10%), H-5→L+5 (10%), H-5→L+6 (21%)	ICT, π -π*

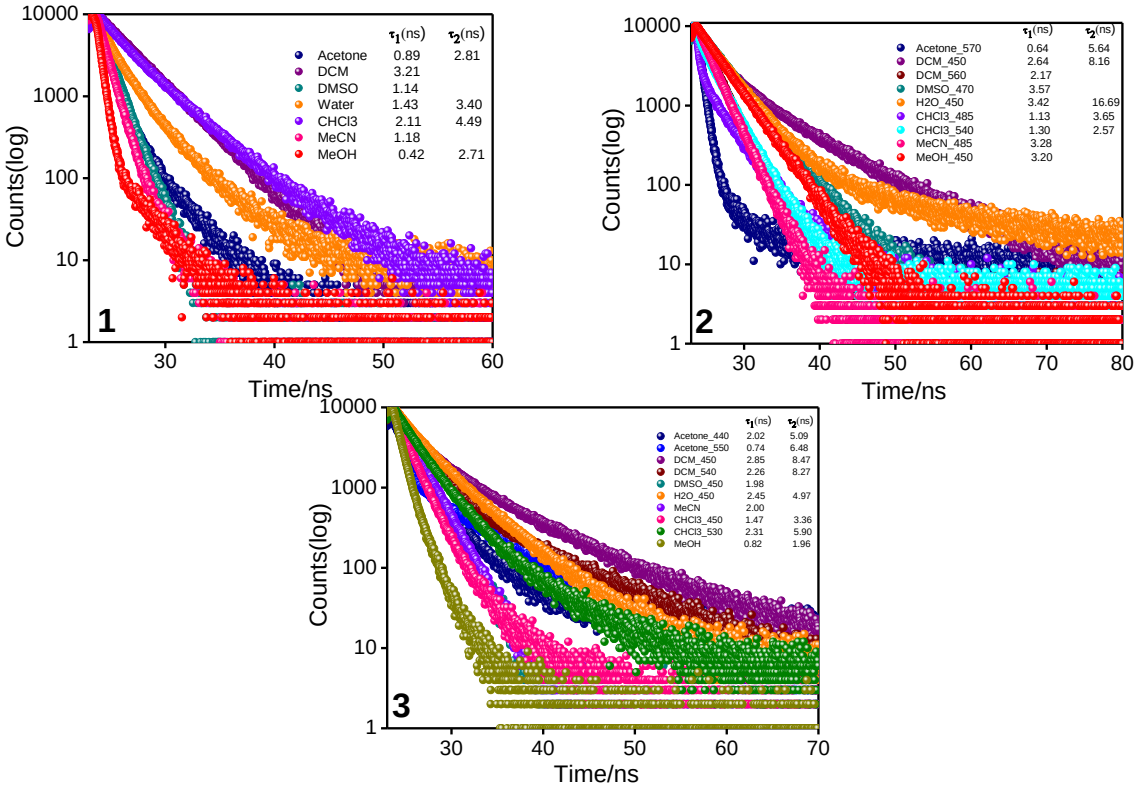

Fig. S19 Time-resolved emission decays (λ_{ex}=370 nm) of **1-3** in different solvent. The inset represents their lifetimes.

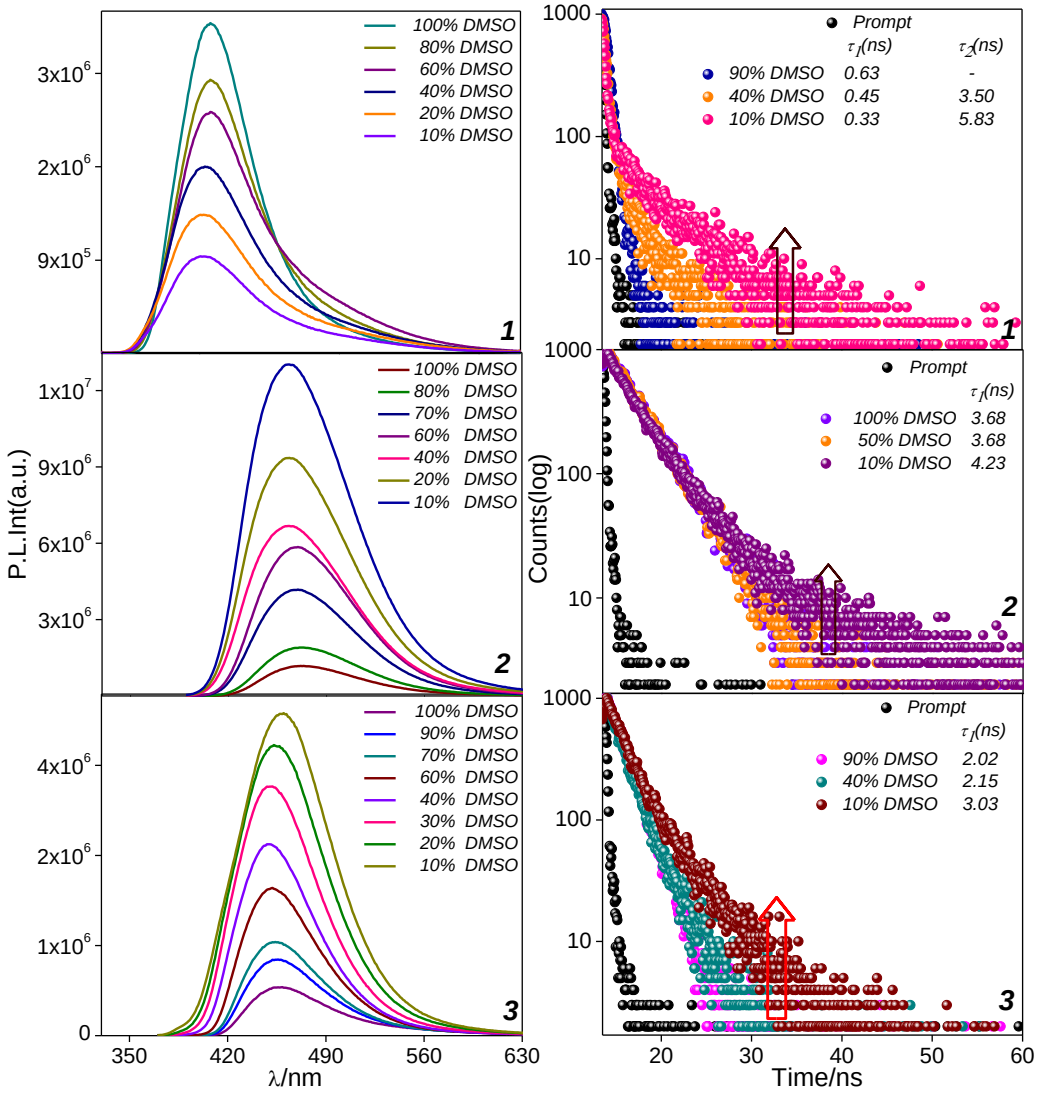

Fig. S20 Aggregation-induced emission (λ_{ex}=350 nm) enhancement upon increasing the ratio of water in DMSO solution of **1-3** (left panel). Corresponding change in emission decays and lifetime is presented in the right panel.

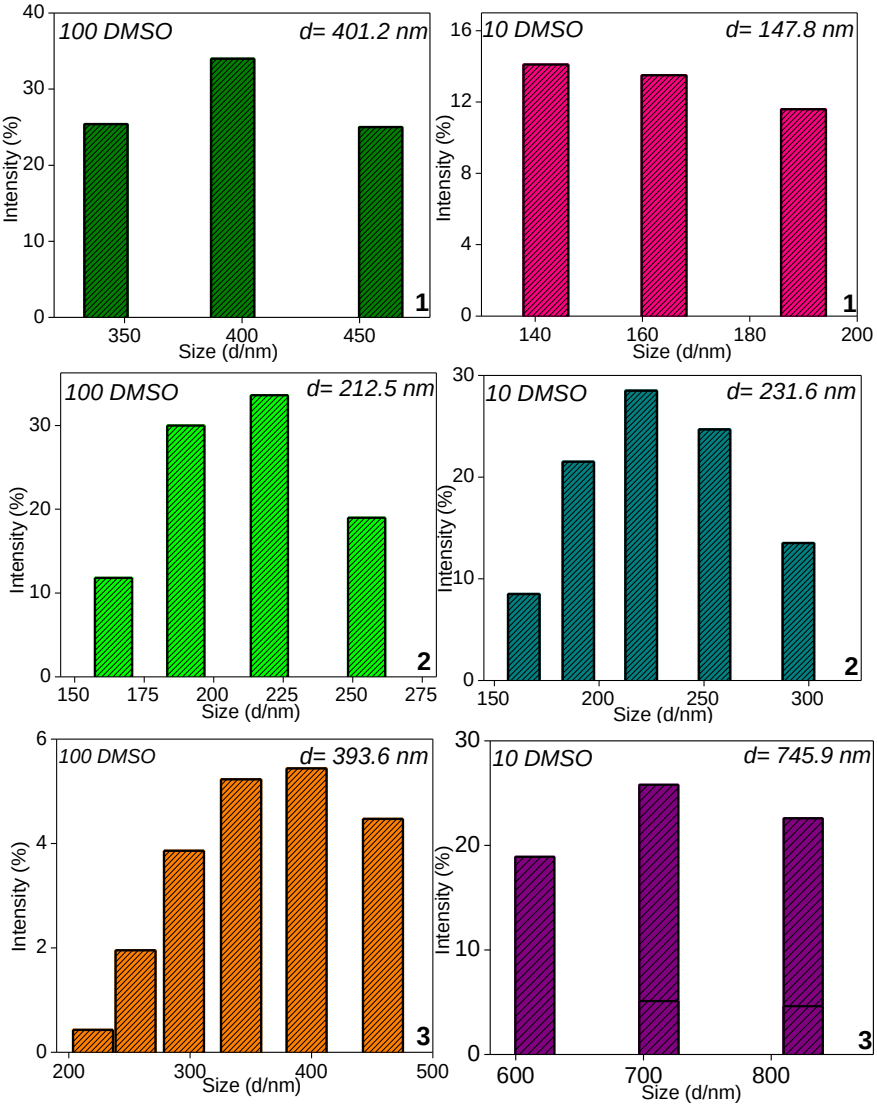

Fig. S21 DLS data **1-3** in DMSO-H_2O mixture.

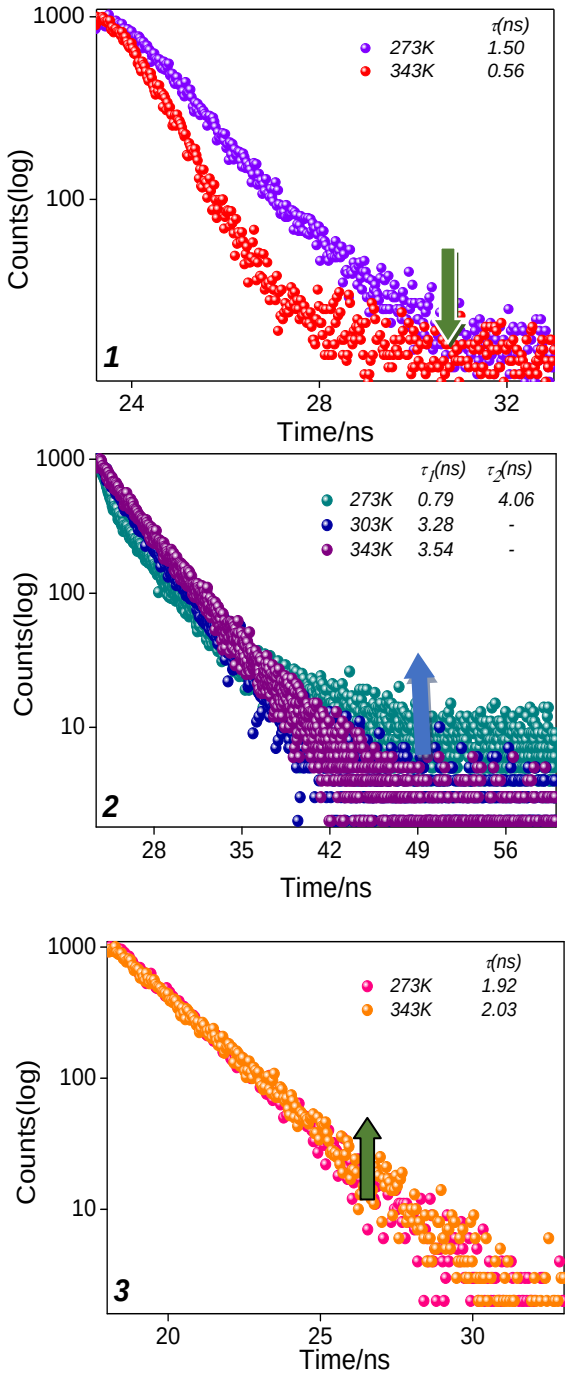

Fig. S22 Temperature-dependent emission decay profiles (λ_{ex} = 370 nm) of **1-3** in acetonitrile recorded in the temperature range 268K-343K, monitored at their respective emission maxima. The corresponding lifetime values at different temperatures are shown in the insets.

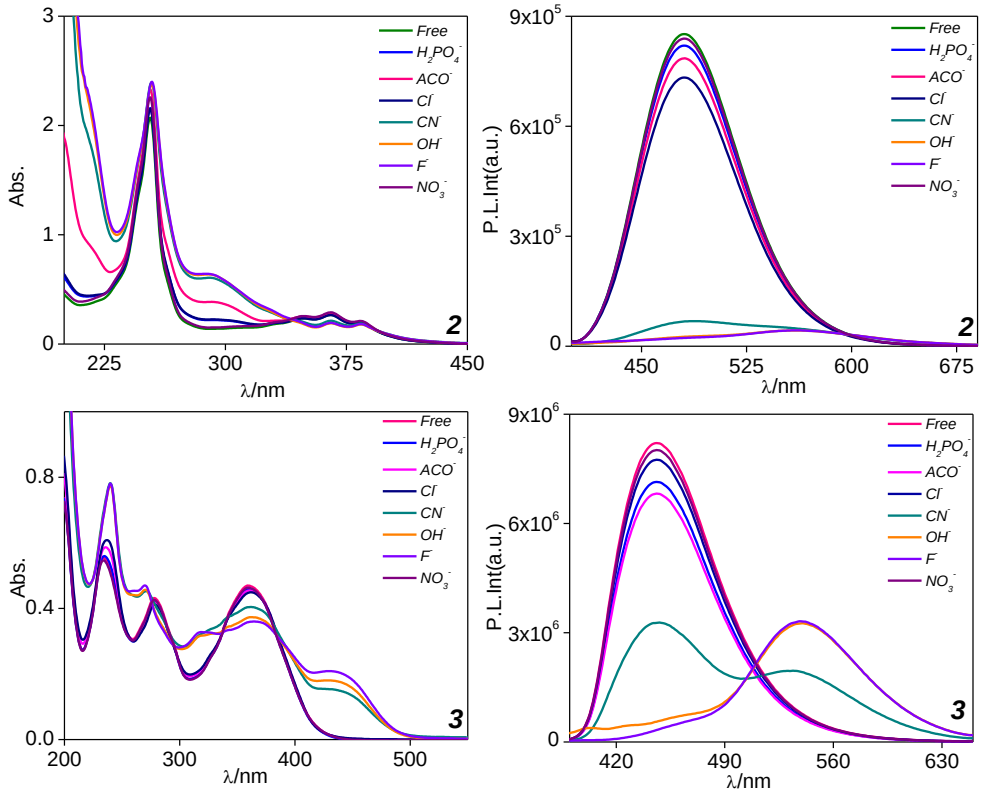

Fig. S23 Absorption (left panel) and emission (right panel) (λ_{ex}=370 nm) spectral response of **2** and **3** in presence of anions.

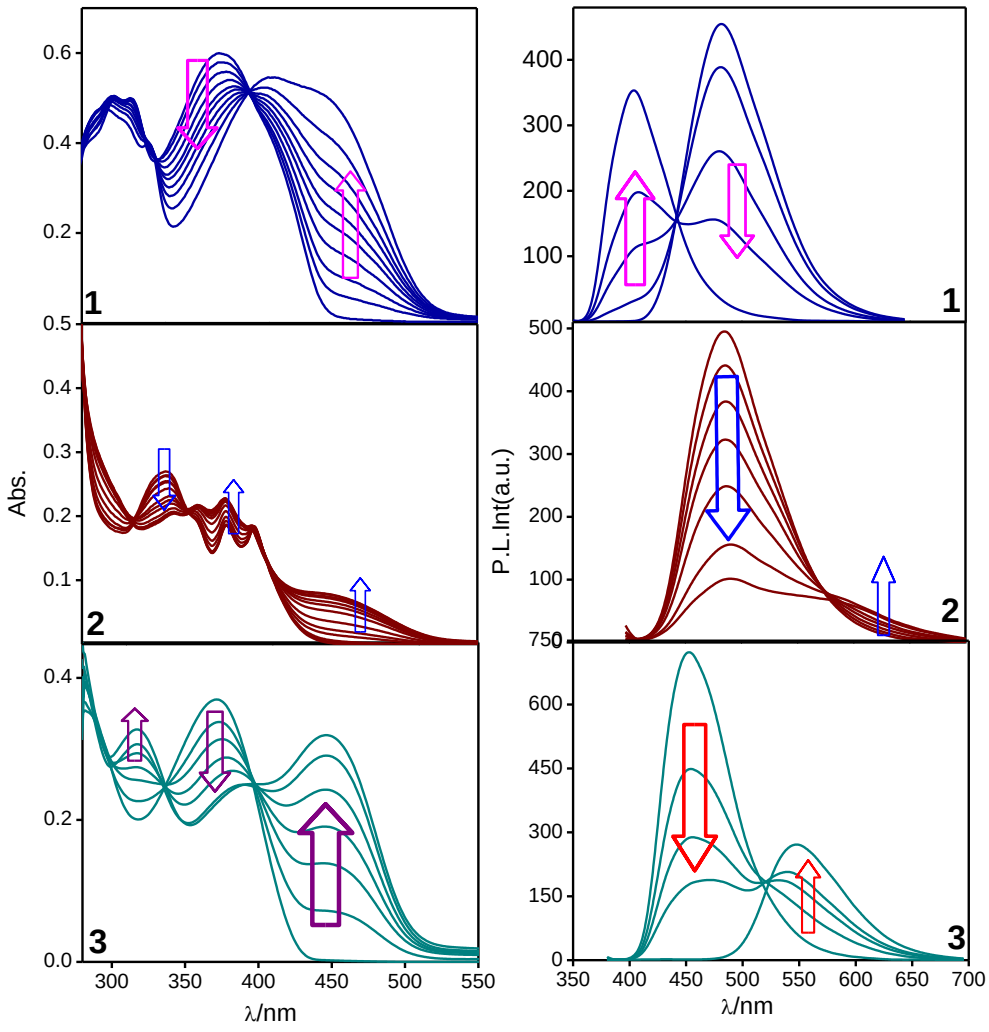

Fig. S24 Absorption (left panel) and emission (λ_{ex}=350 nm) (right panel) spectral profiles of **1**-**3** in MeCN upon gradual addition of OH^-.

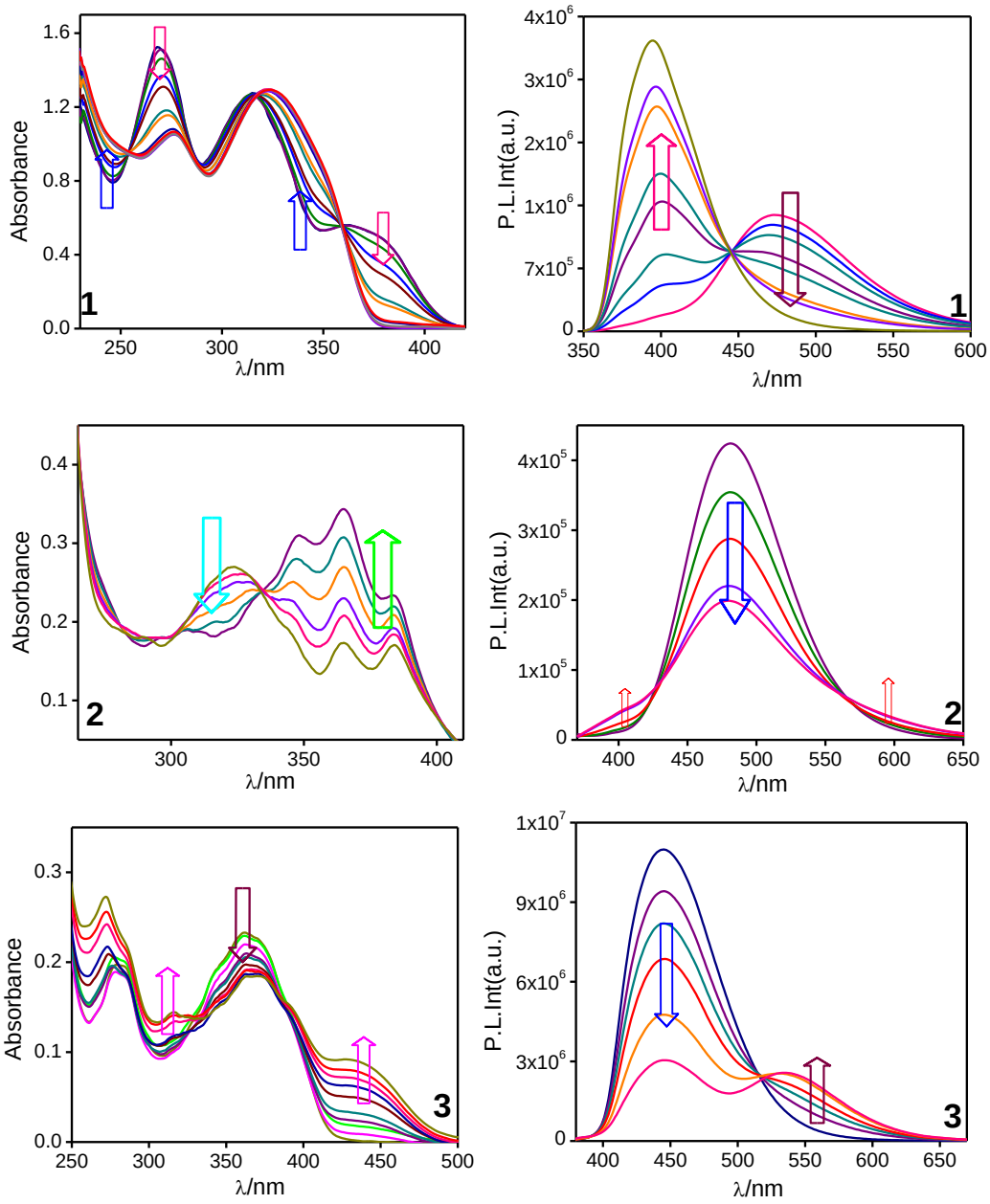

Fig. S25 Absorption (left panel) and emission (λ_{ex}=350 nm) (right panel) spectral profiles of **1**-**3** in MeCN upon gradual addition of CN^-.

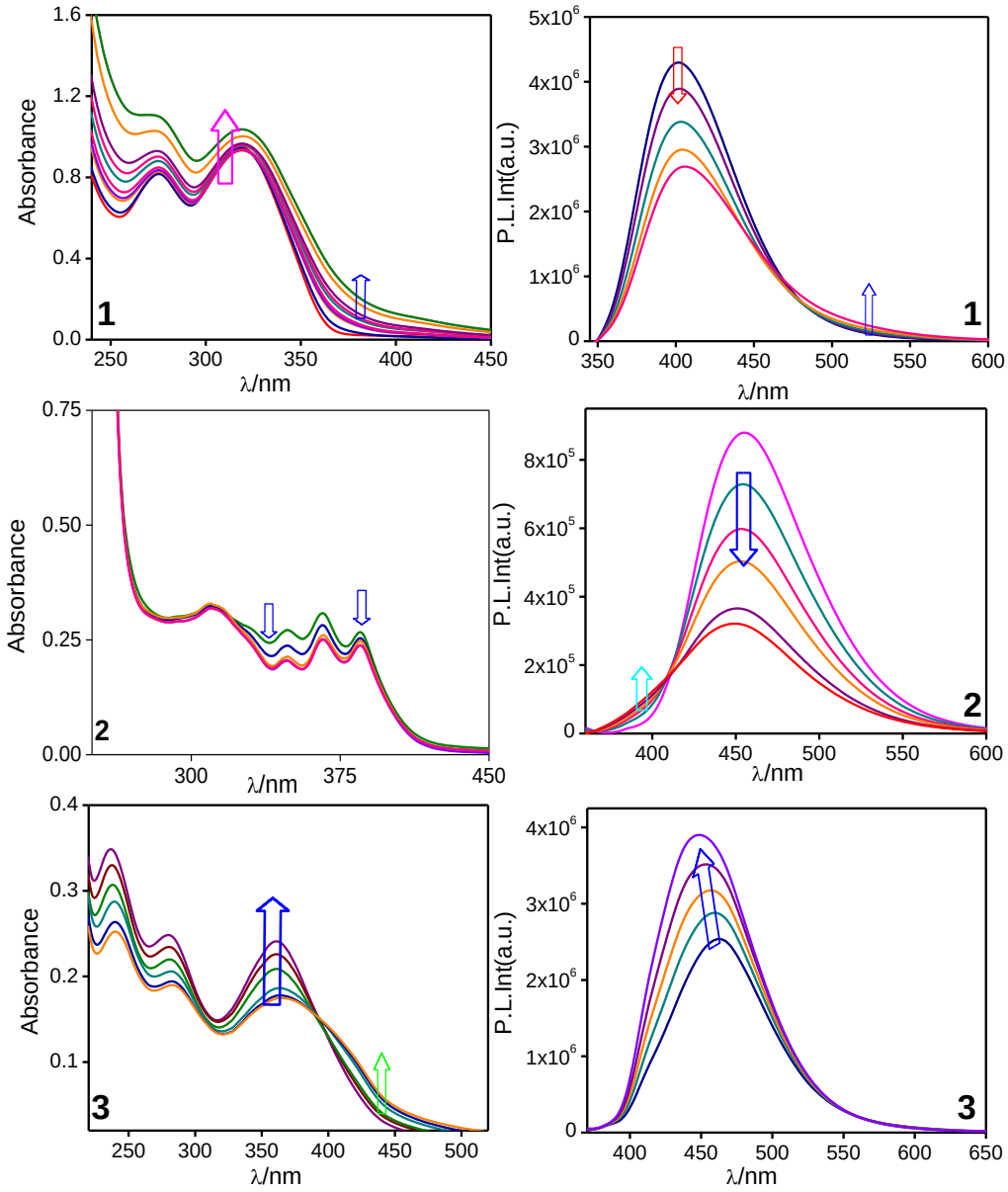

Fig. S26 Absorption (left panel) and emission (λ_{ex}=350 nm) (right panel) spectral profiles of **1**-**3** in water upon gradual addition of CN^-.

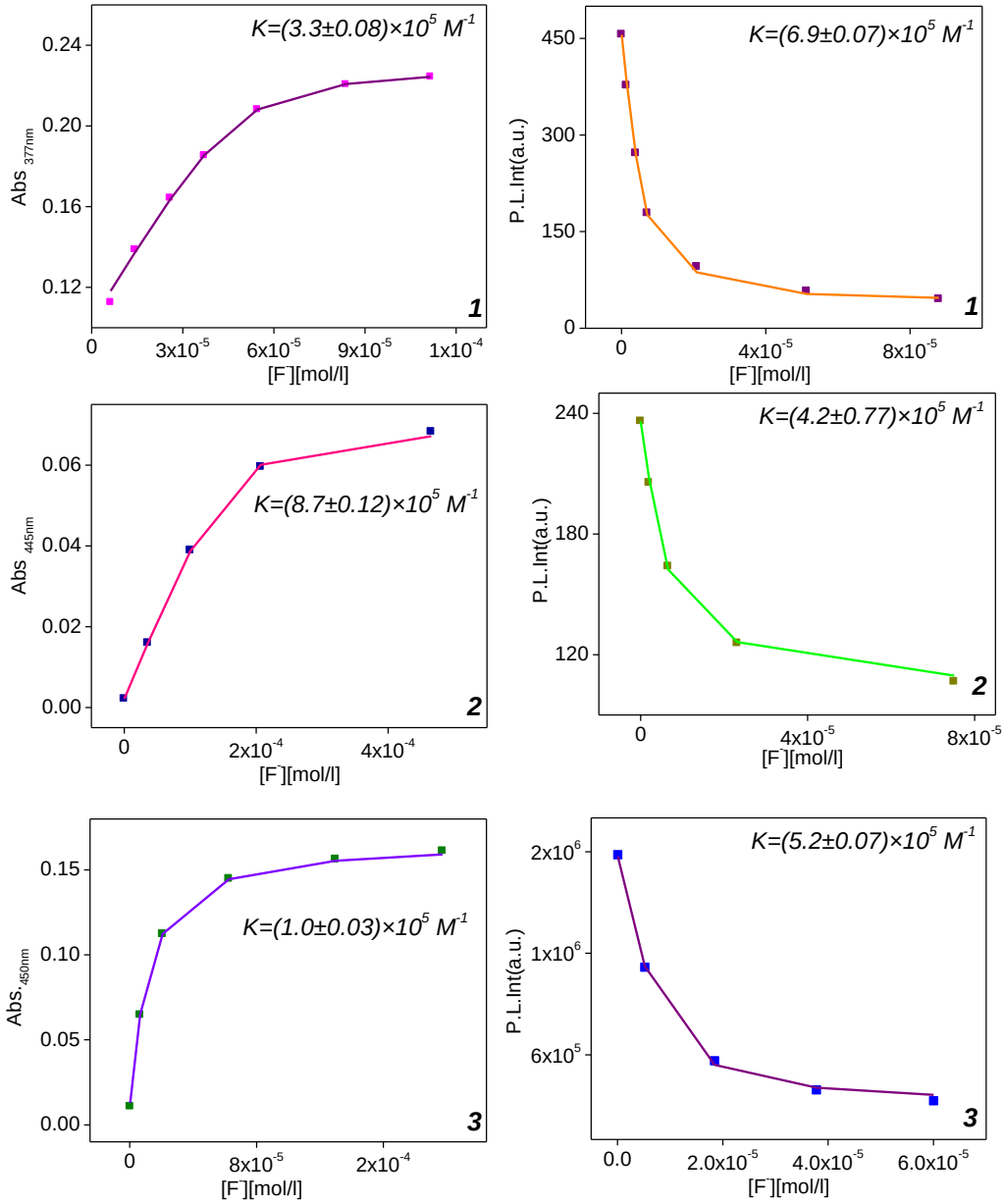

Fig. S27 Absorption and emission spectral changes during the titration of the receptors **1-3** (2.0×10^{-5} M) with F^- in MeCN. The calculated binding constant of receptor are 3.3×10^5 M^{-1} for **1,** 8.7×10^5 M^{-1} for **2** and 1.0×10^5 M^{-1} for **3** from absorption spectral profiles, while respective value is 6.9×10^6 M^{-1}, 4.2×10^5 M^{-1} and 5.2×10^6 M^{-1} for emission spectral profiles.

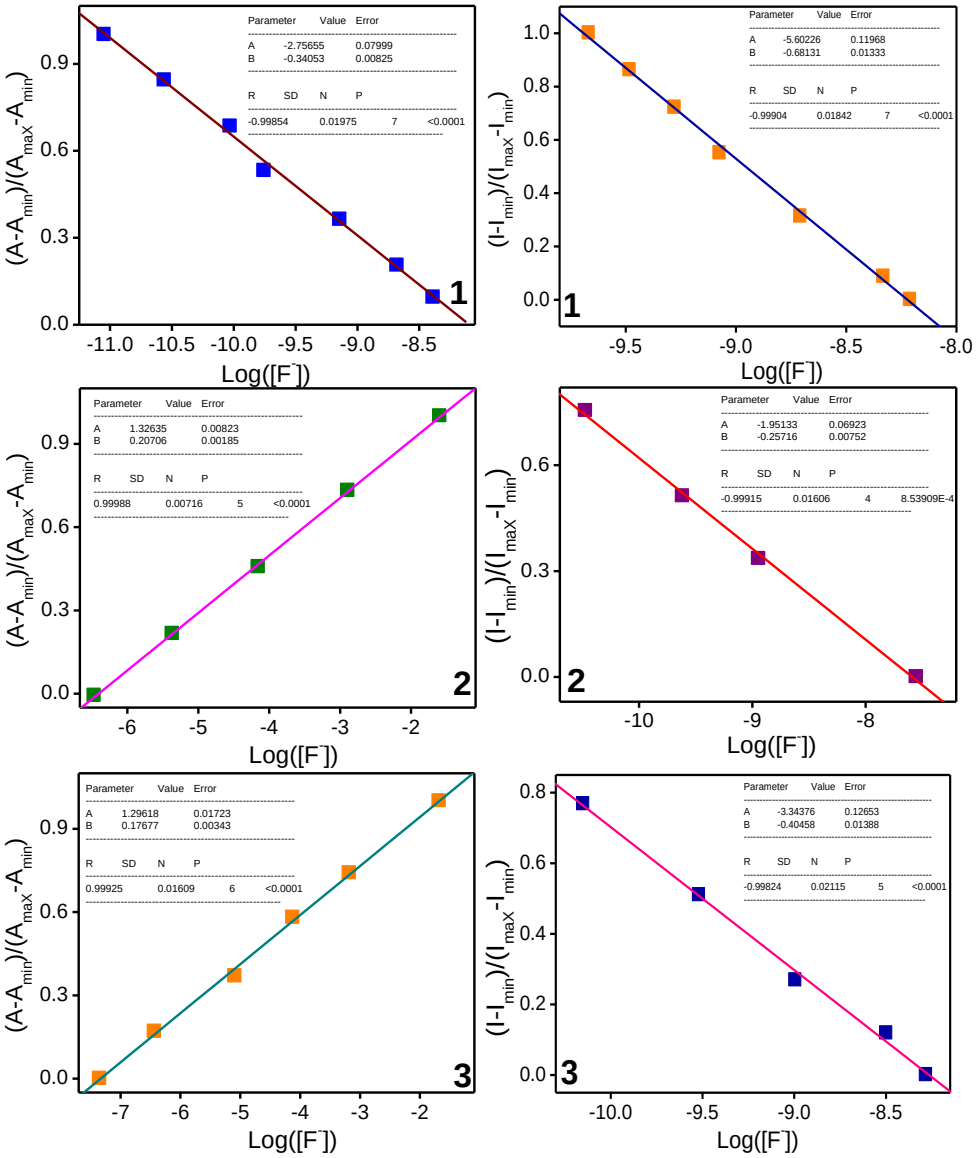

Fig. S28 Absorption and emission spectral changes during the titration of the receptors **1-3** (2.0×10^{-5} M) with F^- in MeCN. (a) Plot of $(A-A_{min})/(A_{max}-A_{min})$ vs. Log ($[F^-]$), gives rise to the detection limit of receptor 1.58×10^{-8} M, 1.99×10^{-7} M and 3.16×10^{-8} M for **1**, **2**, and **3**, respectively. (b) The plot of $(I-I_{min})/(I_{max}-I_{min})$ vs. Log ($[F^-]$) provides the detection limit of receptors 8.31×10^{-9} M for **1**, 5.00×10^{-8} M for **2** and 1.01×10^{-9} M for **3**.

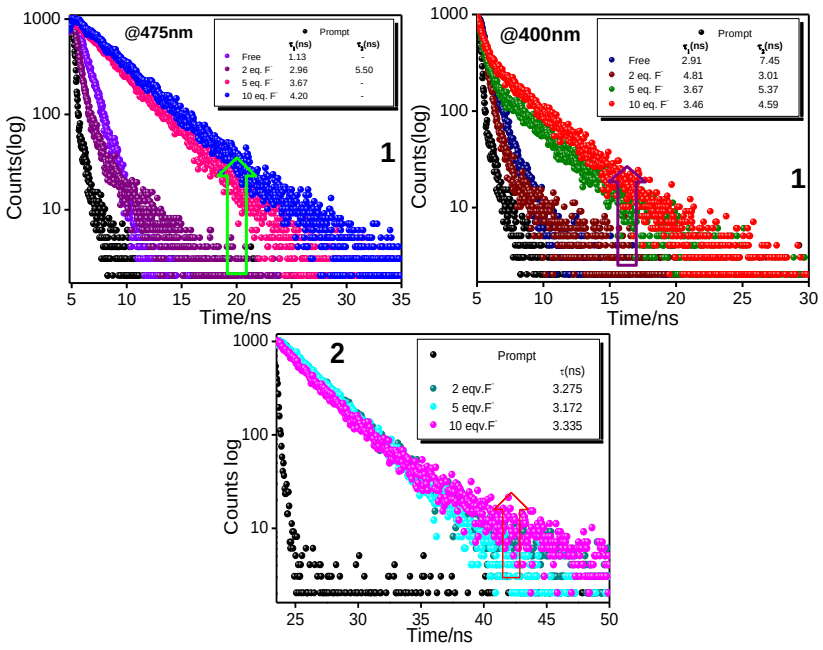

Fig. S29 The change in the emission decays (λ_{ex}=370 nm) of **1** and **2** in acetonitrile upon gradual addition of F^- upon monitoring at 400 and 475 for **1** and 485 nm for **2**. Lifetimes are provided in the respective inset.

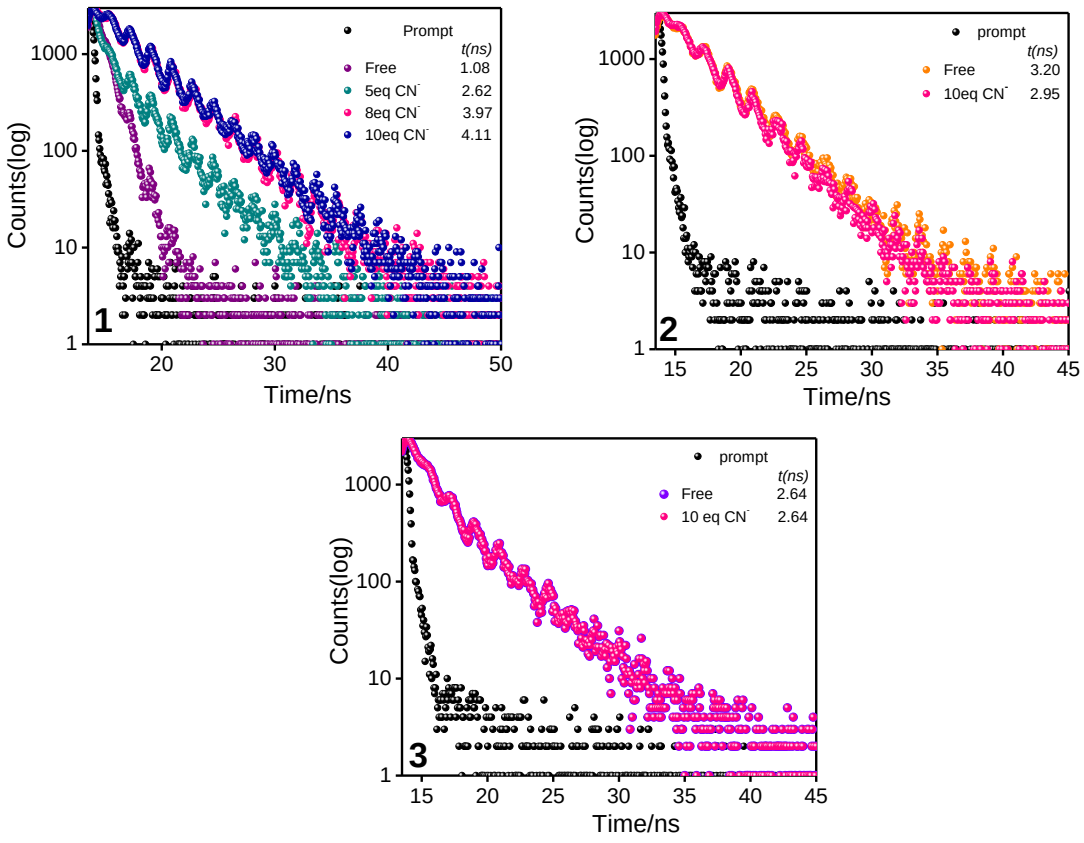

Fig. S30 The change in the emission decays (λ_{ex}=370 nm) of **1-3** in acetonitrile upon gradual addition of CN^- upon monitoring at the respective the emission maxima. Lifetime values are presented in the respective inset.

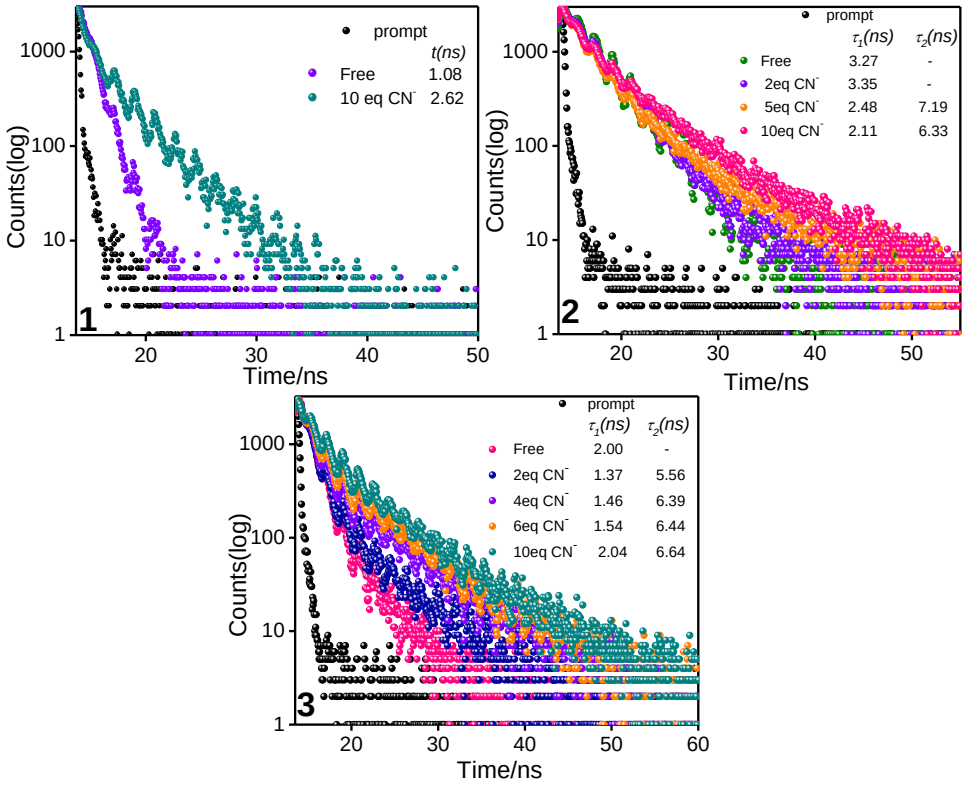

Fig. S31 The change in the emission decays (λ_{ex}=370 nm) of **1-3** in water upon gradual addition of CN^- upon monitoring the emission maxima. Lifetime values are presented in the respective inset.

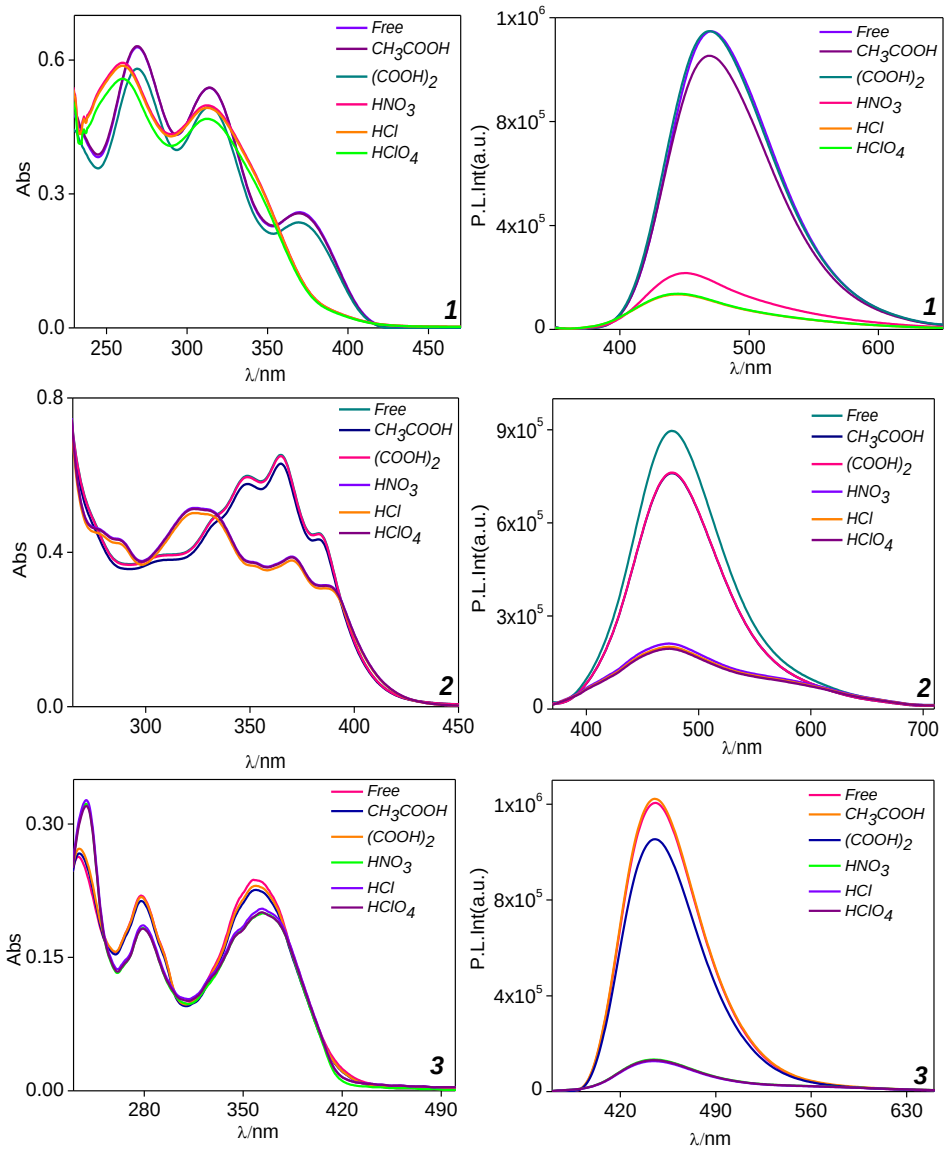

Fig. S32 Absorption (left column) and emission (right column) (λ_{ex} =350 nm) spectral response of **1-3** in presence of different acids in MeCN.

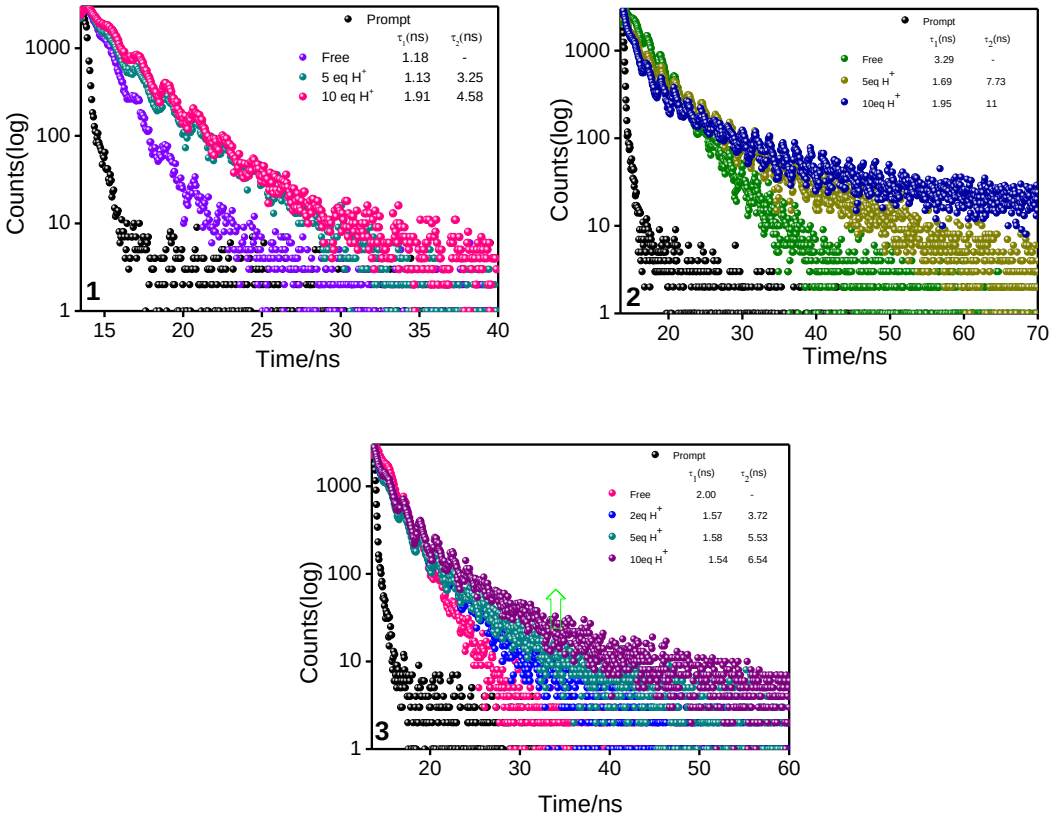

Fig. S33 The change in the emission decays (λ_{ex}=370 nm) of **1-3** in acetonitrile upon gradual addition of H^+ upon monitoring at their respective emission maxima. Lifetime values are provided in the respective inset.

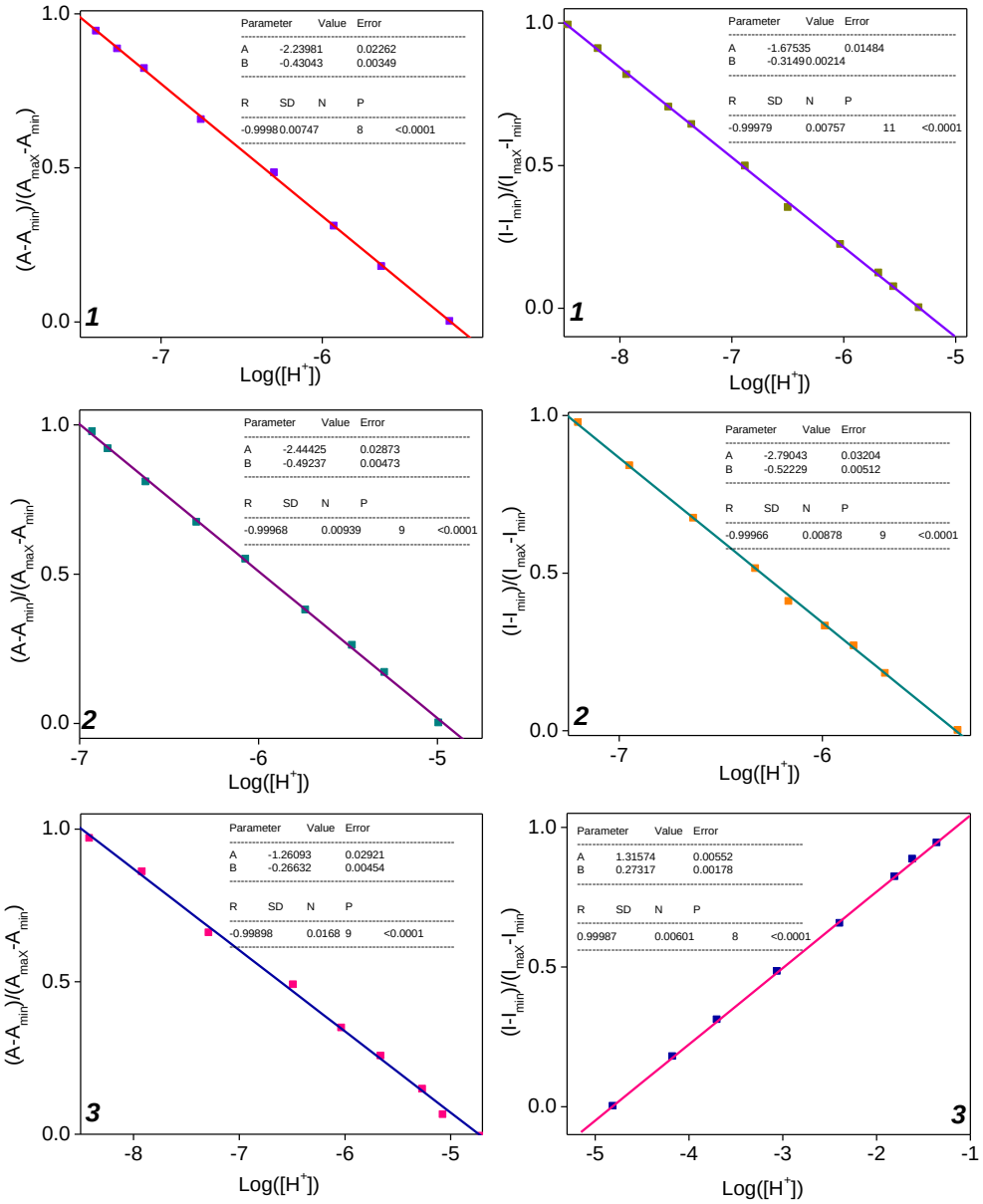

Fig. S34 Absorption and emission spectral changes during the titration of the receptors **1-3** (2.0×10^{-5} M) with H^+ in MeCN. Plot of $(A-A_{min})/(A_{max}-A_{min})$ vs. Log ($[H^+]$), gives rise to the detection limit of receptor 8.3×10^{-6} M, 1.3×10^{-5} M and 1.8×10^{-5} M for **1**, **2**, and **3**, respectively. The plot of $(I-I_{min})/ (I_{max}-I_{min})$ vs. Log ($[H^+]$), provides the detection limit of receptors 1.0×10^{-5} M for **1**, 5.00×10^{-6} M for **2** and 7.0×10^{-6} M for **3**.

Notes and references

(S1) K. Nakamaru, *Bull. Chem. Soc. Jpn.*, 1982, **55**, 1639-1640.

(S2) A. D. Becke, *J. Chem. Phys.*, 1993**, 98**, 5648-5652.

(S3) C. T. Lee, W. T. Yang, R. G. Parr, *Phys. Rev. B.*, 1988, **37**, 785-789.

(S4) P. J. Hay, W. R. Wadt, *J. Chem. Phys.*, 1985, **82**, *299-310*.

(S5) M. E. Casida, C. Jamorski, K. C. Casida, D. R. Salahub, *J. Chem. Phys*., 1998, **108**, 4439-4449.

(S6) R. E. Stratmann, G. E. Scuseria, M. J. Frisch, *J. Chem. Phys*., 1998, **109**, 8218-8224.

(S7) V. A. Walters, C. M. Hadad, Y. Thiel, S. D. Colson, K. B. Wiberg, P. M. Johnson, J. B. Foresman, *J. Am. Chem. Soc*.**,** 1991, **113**, 4782-4791.

(S8) M. Caricato, B. Mennucci, J. Tomasi, F. Ingrosso, R. Cammi, S. Corni, G. J. Scalmani, *Chem. Phys.* 2006, **124**, 124520-124533.

(S9) B. Mennucci, C. Cappelli, C. A. Guido, R. Cammi, J. Tomasi, *J. Phys. Chem. A*, 2009, **113**, 3009-3020.

(S10) R. I. I. Dennington, T. Keith, J. Millam, *Gauss View 3*., 2007.

(S11) N. M. O Boyle, A. L. Tenderholt, K. M. Langner, *J. Comput. Chem.* 2008, **29**, 839-845.